Synthesis, DNA binding studies, and antiproliferative activity of novel Pt(II)-complexes with an L-alanyl-based ligand

Claudia Riccardi[a§], Domenica Capasso[b§], Giovanna M. Rozza[a], Chiara Platella[a],

Daniela Montesarchio[a], Sonia Di Gaetano[c], Tiziano Marzo[d],

Alessandro Pratesi[e], Luigi Messori[e], Giovanni N. Roviello[c,*], Domenica Musumeci[a,c,*]

[a] *Department of Chemical Sciences, University of Napoli Federico II, 80126, Napoli, Italy;*

[b] *Department of Pharmacy, University of Napoli Federico II, 80131, Napoli, Italy;*

[c] *CNR, Institute of Biostructure and Bioimaging, 80134 Napoli, Italy;*

[d] *Department of Pharmacy, University of Pisa, 56126, Pisa, Italy;*

[e] *Department of Chemistry Ugo Schiff, University of Firenze, 50019 Sesto Fiorentino, Italy.*

*Correspondence to:

Domenica Musumeci, *Department of Chemical Sciences, University of Napoli Federico II, Via Cintia, 21, I-80126 Napoli, Italy*

E-mail address: domenica.musumeci@unina.it

Phone: +39-081-674143;

and

Giovanni N. Roviello, *CNR - Institute of Biostructure and Bioimaging, 80134 Napoli, Italy*

E-mail address: giroviel@unina.it

§ These authors contributed equally to this work

Abstract

An artificial alanine-based amino acid (S)-2-amino-3-(4-propyl-3-(thiophen-2-yl)-5-thioxo-4,5-dihydro-1*H*-1,2,4-triazol-1-yl)propanoic acid, named *TioxAla*}, bearing a substituted triazolyl-thione group on the side chain and able to bind RNA biomedical targets, was here chosen as a valuable scaffold for the synthesis of new platinum complexes with potential dual action owing to the concomitant presence of the metal centre and the amino acid moiety. Three new platinum complexes, obtained from the reaction of *TioxAla* with K_2PtCl_4, were characterized by mass spectrometry, NMR and UV-vis spectroscopy: one compound (**Pt1**) consisted of two amino acid units coordinating the Pt(II) ion; the other two, **Pt2** and **Pt3**, were isomers including in their structure one *TioxAla* unit, and two chlorides as Pt-ligands. Pt coordination involved preferentially the amino, carboxylic and thione functions of *TioxAla*. By preliminary antiproliferative assays, a moderate cytotoxic activity on cancer cells was observed only for **Pt2** and **Pt3**, and not for the chloride-free complex (**Pt1**), nor for *TioxAla*. This cytotoxicity, however lower than that of cisplatin, related with the marked ability, here found only for **Pt2** and **Pt3** complexes, to bind DNA sequences either in random coil or in structured forms (duplex and G-quadruplex), as verified by spectroscopic and spectrometric analysis.

1. Introduction

Cisplatin (*cis*-[PtCl$_2$(NH$_3$)$_2$], CDDP), as well as its analogues carboplatin and oxaliplatin, are the most widely employed chemotherapeutic agents,[1] highly effective in the treatment of several tumours including bladder, head, neck, lung, ovarian, and testicular cancers.[2] Once within cell, cisplatin reacts with the nucleophilic groups of the cellular components and efficiently binds DNA, which emerged as the main target accounting for cisplatin antitumor activity.[3,4] Platination of DNA essentially involves metal coordination to the N-7 position of purine bases, generally two contiguous guanines (**G**s) or adjacent **G**s and adenines (**A**s) on the same strand (intrastrand cross-linking).[5] These events give rise to about 60% and 30% of the overall DNA metallation sites, respectively.[5]

Extensive use of cisplatin is however restricted because of drug resistance and severe dose-limiting side effects, such as nephrotoxicity, neurotoxicity, ototoxicity and myelosuppression.[2] Therefore, in the search for innovative and more effective metal-based drugs, a great interest has been devoted to the design and synthesis of novel and even unusual cisplatin analogues displaying a wide range of anticancer activities and concomitantly overcoming cisplatin drawbacks.[3,6]

A great number of cisplatin-like complexes or their trans analogues have been investigated thus far. In most cases, platinum complexes contained heteroaromatic ligands such as pyridine or its derivatives,[7–9] imidazoles,[10,11] thiazole,[7] pyrazoles,[12,13] quinoline and isoquinoline,[7] tetrazoles and triazoles.[14]

Furthermore, sulfoxides and, more in general, sulfur-containing compounds are also interesting as Pt ligands since the Pt-S bond has both a ligand-to-metal σ donation character and a metal-to-ligand π-backdonation. Several platinum complexes containing sulfoxide groups have been indeed proposed as new antineoplastic drugs.[15,16] In particular, various complexes prepared starting from alkyl esters of β-hydroxyditiocinnamic acid (O,S-bidentate) showed promising cytotoxic activity - assessed on the cisplatin-resistant lung tumour cell line - with significant effects at low μM concentrations, accompanied by considerable reactivity towards peptides and model proteins (cytochrome c, albumin, lysozyme, glutathione) as well as DNA.[17,18]

In addition, Pt(II) can form stable complexes with amino acids or diamino acids by exploiting both the amino and carboxylic function in α position, or one of these groups in combination with a side-chain moiety.[19] For example the non-proteinogenic amino acid L-2,3-diaminopropanoic acid (**DAPA**) and its derivatives provide Pt(II) complexes with a planar square structure in which both its amino groups or the α-amino and carboxylic functions (N,N or N,O interactions) are linked to Pt forming a 5-membered ring.[20–22] The platinum complexes of **DAPA** are also able to form intrastrand adducts with DNA and distort its double helix, showing cytotoxic activity in cancer cell lines in a dose- and time-dependent manner.[21]

Few years ago, Saghyan et al. synthesized a new artificial amino acid based on L-alanine, bearing on the side chain a triazolyl-thione group substituted on the triazole ring by a thiophenyl and a propyl moiety (**Fig. 1**).[23] Notably, by UV and CD experiments we previously proved the ability of this heteroaromatic amino acid to bind RNA, interesting aspect in biomedical strategies based on modulation of RNA-RNA molecular recognition.[23] This artificial alanine-based amino acid, named *TioxAla* (**Fig. 1**), has been here selected as a valuable scaffold for the synthesis of new Pt(II) complexes. Indeed, *TioxAla* could represent a suitable ligand in the preparation of Pt(II)-based analogues, exhibiting in its structure various sites potentially able to coordinate platinum ions (i.e. the sulfur of the thione or thiophene moieties, the oxygens of the carboxylic group, the nitrogen of

the α-amino function). Thus, the resulting complexes may exert a synergic activity due to the concomitant presence of the metal and the amino acid.

The reaction between *TioxAla* and the commercially available K_2PtCl_4 platinum salt has been performed in two experimental conditions, leading to different platinum complexes (**Pt1**, **Pt2** and **Pt3**, **Fig. 1**). All the obtained Pt(II)-based compounds have been characterized by mass spectrometry, NMR and UV-vis spectroscopy and their molecular structure elucidated. A detailed UV-vis analysis of all the Pt(II) complexes in different conditions was performed in order to evaluate their stability over time and absorption features in comparison with the starting amino acid.

The ability of the new Pt(II) complexes to bind DNA, in analogy to other metal complexes, was explored using UV and CD spectroscopic measurements as well as ESI-MS analysis on different DNA model systems, both in random coil and in structured forms.

Finally, the antiproliferative activity of the new Pt(II) complexes has been tested on different cancer and normal human cell lines, using cisplatin as a positive control.
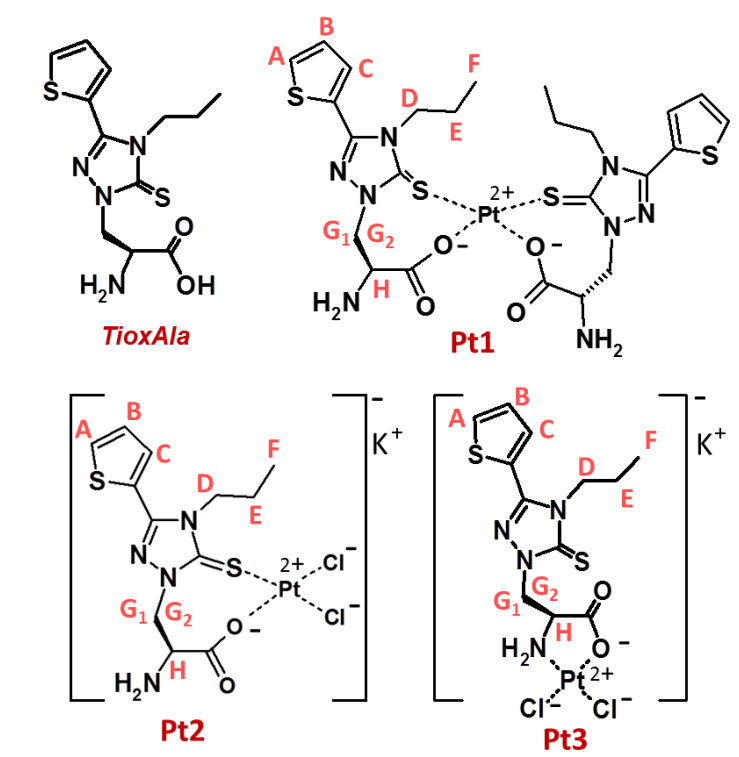
Figure 1: Molecular structure of the artificial amino acid, here named *TioxAla*, based on L-alanine derivatized with a triazolyl-thione group and a thiophenyl moiety. Structures assigned to the three novel complexes **Pt1**, **Pt2** and **Pt3** with the symbolism used for the NMR assignments.

2. Experimental Section

2.1. Materials and general methods

All the reagents and solvents were of the highest commercially available quality and were used as received. TLC (Thin Layer Chromatography) analyses were carried out on silica gel plates from Macherey-Nagel (60, F254) and reaction products on TLC plates were visualized by UV light.

NMR spectra were recorded on Bruker Avance III HD 400 or Varian Inova 500 MHz spectrometers, as specified. All chemical shifts (δ) are reported in ppm and all coupling constants (J) are expressed in Hertz (Hz). The following abbreviations were used for the multiplicity of the NMR resonances: d = doublet, dd = doublet of doublets, t = triplet, m = multiplet; b = broad.

MALDI-TOF mass spectrometric analyses were performed on a TOF / TOF ™ 5800 System in positive ion mode, using α-cyano-hydroxycinnamic acid (CHCA) as matrix.

High resolution (HR) ESI mass spectra were acquired with an AB SCIEX TripleTOF 5600+ mass spectrometer, operating in positive or negative ion mode. Eperimental errors were reported for each compound.

The UV-vis measurements were performed at 20 °C on a JASCO V-550 UV-vis spectrophotometer equipped with a Peltier Thermostat JASCO ETC-505T, by using both a 1-cm path length cuvette (1 mL internal volume, Hellma) and a two-chambers cell (2x0.4375 cm path length, 2 mL internal volume, Hellma). The spectra were recorded with a medium response, a scanning speed of 100 nm/min and a 2.0 nm bandwidth with the appropriate baseline subtracted. Each experiment was performed in triplicate.

CD spectra were recorded at 20 °C on a Jasco J-715 spectropolarimeter equipped with a Peltier-type temperature control system (model PTC-348WI). The spectra were recorded with a response of 1 s, a scanning speed of 100 nm/min and a 2.0 nm bandwidth. All the spectra were averaged over 3 scans and each experiment performed in triplicate.

UV and CD binding experiments were performed in the two-chambers cell, that is a quartz cuvette with two partially separated compartments and an optical path length of 0.875 cm (0.4375 cm *per* chamber). First, the *sum* spectrum of the two separated components inserted in the two compartments of the cuvette were recorded, and, subsequently, by turning up and down the cell, the spectrum obtained after mixing the solutions (*mix*), registered at different times, accordingly with previous works.[24,25]

2.2. Synthesis and characterization of the amino acid derivative

The amino acid derivative *TioxAla* (**Fig. 1**) was synthesized as previously decribed[23] (white powder) and characterized by mass, NMR and UV-vis techniques (**Figs. S1** and **S2**).

TLC: R_f = 0.25 (CH$_2$Cl$_2$/CH$_3$OH, 8:2 v/v).

HR ESI-MS: measured *m/z* 313.0803 [M+H]$^+$; calculated *m/z* for C$_{12}$H$_{16}$N$_4$O$_2$S$_2$ [M+H]$^+$ 313.0787; error 5.1 ppm (**Fig. S1**, bottom-right).

^{1}H NMR (400 MHz, CD$_3$OD, **Fig. S1**, top): δ 7.75 (dd, J = 5.1, 1.1 Hz, 1H, A), 7.64 (dd, J = 3.8, 1.1 Hz, 1H, C), 7.25 (dd, J = 5.1, 3.8 Hz, 1H, B), 4.93 (dd, J = 14.4, 4.1 Hz, 1H, G$_1$), 4.69 (dd, J = 14.4, 7.6 Hz, 1H, G$_2$), 4.63 (dd, J = 7.6, 4.1 Hz, 1H, H), 4.23 (m, peak with = 0.115 ppm, 2H, D), 1.82 (m, peak with = 0.096 ppm, 2H, E), 0.96 (t, J = 7.4 Hz, 3H, F).

^{13}C NMR (125 MHz, CD$_3$OD, **Fig. S1**, middle): 170.2 (COOH); 169.1 (C=S); 147.8 (N-C=N); 131.1 (A); 131.0 (C); 129.3 (B); 127.2 (S-$\underline{C}$=C); 52.9 (H); 49.0 (G); 48.5 (D); 22.5 (E); 11.2 (F). 1% CF$_3$COOH (v/v) was added in the NMR cuvette to improve sample solubility.

2.3. Synthesis and characterization of the novel platinum-based complexes

2.3.1. Synthesis and characterization of Pt1

In a first complexation reaction, the amino acid *TioxAla* (2 equiv., 8.3 mg, 26.6 µmol), suspended in 800 µL acetone (white suspension), was slowly added in 1 h to a solution of potassium tetrachloroplatinate (K$_2$PtCl$_4$, 1 equiv., 5.5 mg, 13.3 µmol), dissolved in the minimum amount of H$_2$O (final acetone/H$_2$O ratio = 75:25, v/v). The reaction mixture was kept protected from light, under stirring for about 3 h, until the formation of a yellow suspension from the initial dark-orange/white suspension. Then, the solvent was removed under vacuum at 30 °C and the reaction crude was further dried for 1 h at the oil pump to remove traces of H$_2$O. After this, it was resuspended with cold methanol recovering a clear yellow solution which contained a single pure product (9.9 mg, yellow powder, 91% yield) identified as **Pt1** (**Fig. 1**) by MALDI-TOF MS (**Figs. 2a** and **S3**), ESI-MS (**Fig. S4**) and NMR analyses (**Fig. S5** and **S6**).

Pt1 was partially soluble in acetone and CH$_2$Cl$_2$, and showed a good solubility in CH$_3$OH. Attempts to obtain crystals of **Pt1** suitable for X-ray crystallography were unsuccessful, always giving an amorphous yellow solid.

MALDI-TOF MS: m/z 818.07 (calculated for [**Pt1**+H$^+$]$^+$ = [C$_{24}$H$_{30}$N$_8$O$_4$S$_4$Pt+H$^+$]$^+$ = 818.10), 856.01 (calculated for [**Pt1**+K$^+$]$^+$ = 856.05) (**Fig. 2a**).

HR ESI-MS: measured *m/z* 818.0999 [M+H]$^+$; calculated *m/z* for C$_{24}$H$_{30}$N$_8$O$_4$S$_4$Pt [M+H]$^+$ 818.1019; error 3.1 ppm (**Fig. S4**).

^{1}H NMR (400 MHz, CD$_3$OD, **Fig. S5**, top): δ 7.88 (dd, J = 5.1, 1.1 Hz, 1H, A), 7.74 (dd, J = 3.8, 1.1 Hz, 1H, C), 7.33 (dd, J = 5.1, 3.8 Hz, 1H, B), 5.19 (dd, J = 14.3, 11.7 Hz, 1H, G$_1$), 4.81 (dd, J = 14.3, 3.5 Hz, 1H, G$_2$), 4.28 (m, 2H, peak with = 0.140 ppm, D), 3.85 (dd, J = 11.6, 3.6 Hz, 1H, H), 1.92 (m, peak with = 0.155 ppm 2H, E), 1.03 (t, J = 7.4 Hz, 3H, F).

^{13}C NMR (100 MHz, CD$_3$OD, **Fig. S5**, bottom): δ 172.6 (C=S), 159.1 (COOH), 150.1 (N-C=N), 132.5 (A), 132.3 (C), 129.7 (B), 125.3 (S-$\underline{C}$=C), 61.8 (H), 56.6 (G), 49.7 (D), 23.2 (E), 11.2 (F).

2.3.2. Synthesis and characterization of Pt2 and Pt3

In a second reaction (II) the starting amino acid *TioxAla* (14.9 mg, 47.6 µmol, 0.6 equiv.) was dissolved in acetone and slowly added in 1 h to K$_2$PtCl$_4$ (32.8 mg, 79.4 µmol, 1 equiv.), in turn previously dissolved in the minimum amount of water (200 µL, final acetone/H$_2$O ratio = 75:25, v/v). After 4 h under stirring and protected from light, TLC monitoring showed the complete consumption of the starting amino acid and the formation of a yellow solution with an orange/yellow precipitate. The reaction was then quenched by removing the solvent under vacuum at 30 °C and further drying the reaction crude at the oil pump to remove traces of H$_2$O. After this, the crude mixture was resuspended under sonication in acetone: a yellow solution and a dark yellow precipitate were obtained. After a series of centrifugations and washings of the precipitate (until the supernatant was completely colourless), the combined yellow acetone solutions (ca. 3 x 10 mL) were taken to dryness, while the dark yellow precipitate was resuspended with methanol. In this case, a solution with a more intense yellow colour and pale pink precipitate were obtained. After centrifugation and washing of

the precipitate with methanol (until the supernatant was completely colourless), all the methanol solutions (c.a. 4 x 10 mL) were combined and taken to dryness. The two yellow components (yellow powders) were then analyzed and characterized separately.

The platinum complex recovered with methanol (10.1 mg, 17.5 µmol, 37 % yield) was insoluble in acetone and partially soluble in H_2O and methanol. Attempts to obtain crystals of the complex, suitable for X-ray crystallography, failed, only giving degradation products (white crystals). The complex was thus characterized by MALDI-TOF mass spectrometry and NMR spectroscopy, and identified as **Pt2** (**Fig. 1**).

Pt2 characterization. MALDI-TOF MS: m/z 600.92 (calculated for $[Pt2+H^++Na^+]^+ = [C_{12}H_{15}N_4O_2S_2PtCl_2+H^++Na^+]^+ = 599.96$), 731.43 (calculated for $[Pt2-Cl^-+CHCA+H^+]^+ = 731.05$) (**Fig. 2b**).

HR ESI-MS: measured *m/z* 506.0301 $[M-2Cl]^+$; calculated *m/z* for $C_{12}H_{15}N_4O_2PtS_2$ $[M-2Cl]^+$ 506.0279; error 4.4 ppm (**Fig. S7**).

^{1}H NMR (400 MHz, CD$_3$OD, **Fig. S8**, top): δ 7.89 (dd, $J = 5.1$, 0.9 Hz, 1H, A), 7.75 (dd, $J = 3.8$, 0.9 Hz, 1H, C), 7.33 (dd, $J = 5.1$, 3.8 Hz, 1H, B), 5.27 (dd, $J = 14.5$, 11.1 Hz, 1H, G$_1$), 4.89 (dd, $J = 14.8$, 3.6 Hz, 1H, G$_2$), 4.29 (m, 2H, peak with = 0.135 ppm, D), 4.16 (dd, $J = 11.1$, 3.6 Hz, 1H, H), 1.92 (m, peak with = 0.147 ppm, 2H, E), 1.03 (t, $J = 7.4$ Hz, 3H, F).

^{13}C NMR (101 MHz, CD$_3$OD, **Fig. S8**, bottom) δ 173.0 (C=S), 159.5 (COOH), 150.7 (N-C=N), 133.0 (A), 132.9 (C), 130.2 (B), 125.5 (S-*C*=C), 56.1 (G), 61.2 (H), 50.0 (D), 23.6 (E), 11.6 (F).

The platinum complex recovered with acetone from the reaction II (15.8 mg, 27.4 µmol, 57 % yield) was insoluble in H_2O at mM conc., sufficiently soluble in CH_3OH and showed a quite good solubility in acetone, and was identified by NMR and MALDI-TOF MS analyses as **Pt3**. Attempts to obtain crystals of the complex, suitable for X-ray crystallography, were unsuccessful always giving an amorphous yellow solid or in some cases white crystals (degradation products).

Pt3 characterization. MALDI-TOF MS: m/z 506.00 (calculated for $[Pt3-2Cl^-]^+ = [C_{12}H_{15}N_4O_2S_2PtCl_2-2Cl^-]^+ = 506.03$), 564.95 (calculated for $[Pt3-Cl^-+Na^+]^+ = 564.93$), 600.84 (calculated for $[Pt3+H^+Na^+]^+ = 599.96$), 732.00 (calculated for $[Pt3-Cl^-+CHCA+H^+]^+ = 731.05$) (**Fig. 2c**).

HR ESI-MS: measured *m/z* 506.0309 $[M-2Cl]^+$; calculated *m/z* for $C_{12}H_{15}N_4O_2PtS_2$ $[M-2Cl]^+$ 506.0279; error 6.0 ppm (**Fig. S9**).

^{1}H NMR (400 MHz, CD$_3$OD, **Fig. S10**, top): δ 7.84 (dd, $J = 5.1$, 1.1 Hz, 1H, A), 7.67 (dd, $J = 3.8$, 1.1 Hz, 1H, C), 7.30 (dd, $J = 5.1$, 3.8 Hz, 1H, B), 5.86 (dd, $J = 14.5$, 4.9 Hz, 1H, G$_1$), 5.64 (bm, 1H, NH$_2$), 5.52 (bm, 1H, NH$_2$), 4.81 (dd, $J = 14.6$, 2.1 Hz, 1H, G$_2$), 4.25 (m, 2H, peak with = 0.117 ppm, D), 4.01 (bdd, $J = 4.9$, 2.1 Hz, 1H, H), 1.89 (m, peak with = 0.095 ppm, 2H, E), 1.00 (t, $J = 7.4$ Hz, 3H, F).

^{13}C NMR (100 MHz, CD$_3$OD, **Fig. S10**, bottom): δ 171.0 (C=S), 163.3 (COOH), 150.1 (N-C=N), 132.6 (A), 132.5 (C), 130.0 (B), 125.8 (S-*C*=C), 59.3 (H), 55.5 (G), 49.6 (D), 23.6 (E), 11.6 (F).

Molar extinction coefficients (ε) for *TioxAla* and the three platinum complexes at the specified wavelength (**Fig. 3**) were calculated from the slopes of standard calibration curves, constructed using Beer's law.

2.4. MALDI-TOF mass spectrometry

For the acquisition of MALDI-TOF mass spectra of the Pt complexes, CHCA matrix was the best one for optimal signal/noise ratio: we also used DHB (2,5-dihydroxybenzoic acid) and THAP (2,4,6-trihydroxyacetophenone) with worst results (as also already reported for other platinum complexes[26]). MALDI-TOF mass spectra of all the complexes were acquired using positive ion-mode (negative modalities did not give any result).

The matrix solution was prepared prior to use at the concentration of 5 mM in acetonitrile/water (1:1, v/v). The metal complex was dissolved in methanol/0.9 % NaCl aqueous solution (1:1, v/v) at the concentration of 0.5 mM. Then, 0.5 μL of the metal complex solution was deposited on the plate, immediately followed by the same volume of the matrix solution and proper mixing before drying the components. The mixture was then left to co-crystallize at r.t..

2.5. DNA binding studies

2.5.1. Preparation of the structured DNA model systems

The duplex structure used for the binding studies was obtained by mixing two 12-mer oligodeoxyribonucleotides [**ODN1**: d($^{5'}$CCTCT*GG*TCTCC$^{3'}$); **ODN2**: d($^{5'}$*GG*A*G*ACCA*GA*GG$^{3'}$)] in 1:1 ratio[27] and performing an annealing procedure taking the sample in the selected buffer at high temperature (95 °C) for 5 min, and then leaving it to slowly cool to room temperature. The formation of the duplex was checked by performing a CD spectrum (**Fig. S17a**) and a UV-melting experiment (data not shown).

Also the ODN sequence d($^{5'}$TTAGGGTTAGGGTTAGGGTTAGGGTT$^{3'}$) (tel$_{26}$) was subjected to the annealing procedure in order to allow the formation of the thermodynamically most stable G4 conformation in the selected K$^+$-containing solution. The conformation adopted by tel$_{26}$ after annealing in the buffer used for the solution studies was essentially a hybrid-2 type structure, as evidenced by the comparison of its CD spectrum, reported in **Fig. S17b**, with those reported in the literature for the same sequence under similar conditions.[28,29]

2.5.2. CD and UV binding experiments

For all the binding experiments, in the *sum* spectra, the oligonucleotide concentration in one of the cell chambers was 4 μM in 50 mM KCl, 10 mM Na$_2$HPO$_4$/NaH$_2$PO$_4$, pH = 7.2, containing 20 μl of CH$_3$OH or acetone, and the ligand solution was 40 μM in the same buffer (diluting a 2 mM stock solution in CH$_3$OH for **Pt1** and **Pt2**, and acetone for **Pt3**). In this way the same amount of organic solvent was present in the ODN solution before and after the cuvette mixing, to exclude modifications of the oligonucleotide conformation due to addition of the organic solvent.

2.5.3. ESI-MS experiments

The HR MS characterization of studied compounds were carried out on AB Sciex TripleTof 5600+ high resolution mass spectrometry. Each spectrum was recorded in positive ion mode through direct injection at 7 μL×min^{-1} flow rate, after dilution of compound stock solution (1 mg/mL in CH$_3$OH) to the final concentration of 1 μg/mL in CH$_3$OH and 0.1% (v/v) formic acid was added. In case of compounds Pt2 and Pt3, 10% (v/v) CH$_3$CN was added to the solution before injection in order to improve signal/noise ratio and electrospray stability.

For HR characterization, the ESI source parameters were: Ion Spray Voltage Floating +5500 V, Temperature 25 °C, Ion source Gas 1 (GS1) 30; Ion source Gas 2 (GS2) 0; Curtain Gas (CUR) 20, Declustering Potential (DP) 80 V, Collision Energy (CE) 10 V.

Platinum-complex/oligonucleotide adducts were prepared by adding the selected Pt-complex dissolved in water to the solution of oligonucleotide (10^{-4} M) in water. The final metal-complex/ODN ratio was 3:1. The solutions were incubated for 24 and 48 h at 37 °C.

For the ESI-MS analysis, aliquots were sampled and diluted with LC-MS water to a final ODN concentration of 10^{-6} M, and 1% (v/v) triethylamine was added. The ESI-MS spectra were acquired through direct infusion at 7 μL×min^{-1} flow rate in the mass spectrometer in negative polarity. The ESI source parameters were: Ion Spray Voltage Floating -4500 V, Temperature 400 °C, Ion source Gas 1 (GS1) 40; Ion source Gas 2 (GS2) 30; Curtain Gas (CUR) 25, Declustering Potential (DP) -30 V, Collision Energy (CE) -10 V. For the acquisition, Analyst TF software 1.7.1 (Sciex) was used and the deconvoluted spectra were obtained by using the Bio Tool Kit micro-application v.2.2 embedded in PeakView™ software v.2.2 (Sciex).

2.6. MTT assay

Cervical carcinoma (HeLa), human melanoma (A375) cell lines, and human dermal fibroblasts (HDF) were maintained in DMEM, supplemented with 10% FBS, 2 mM L-glutamine, 100 μg/mL penicillin and 100 μg/mL streptomycin, in a humidified 5% CO$_2$ at 37 °C.[30,31]

Cells were seeded at density of 7000 (HDF) or 3000 cells (for cancer cell lines) for each well (100 μL), in 96-well flat bottom tissue culture microplates, and incubated with the compounds at 37°C for 48 h. All molecules were dissolved in CH$_3$OH (5 mM) except cisplatin, dissolved in 0.9% NaCl aqueous solution (5 mM), and then diluted with medium at the proper concentration.

The medium was removed, then, the compounds solutions at the proper concentration were added (100 μL for well). Controls were prepared with the same volume of CH$_3$OH or 0.9% NaCl solution, added to cells as vehicle. After incubation, MTT assay was performed to evaluate the proliferating cells.[32] The plate was then read with a microplate reader (Enspire Perkin Elmer) at 570 nm. The same method was used to evaluate the IC$_{50}$ of the compounds by Prism software. Each experiment was performed in triplicate and repeated at least 3 times. Statistical significance was analyzed using Student's t test (* $p < 0.05$).

2.7. Annexin V binding assay

Apoptosis was determined assessing phosphatidylserine exposure by annexin V-FITC binding by means of the FITC Annexin V Apoptosis Detection Kit II, accordingly to the manufacturer's instruction,[33,34] 10000 cells were plated in 6-well, incubated with 50 μM conc. of **Pt2** for 48 h and analyzed by flow cytometer (BD FACSCalibur). Propidium iodide (PI) was used as second dye to stain dead cells. Cells cultured in a drug-free medium were used as controls. Analysis was performed using Cell Quest software. Dot with Annexin V−/PI−(low left quadrant), Annexin V+/PI−(low right

quadrant), Annexin V+/PI− (upper right quadrant) and Annexin V+/PI+(upper left quadrant) features represent intact, early apoptotic, late apoptotic and necrotic cells, respectively.

3. Results and Discussion

3.1. Preparation and characterization of the amino acid *TioxAla*

The synthesis of the L-alanyl-based amino acid was carried out as previously described,[23] and the final product was characterized by ^{1}H and ^{13}C NMR as well as MALDI-TOF mass spectrometry (**Fig. S1**; see also **Table S1** for NMR data).

Then, a UV-vis analysis over time of *TioxAla* dissolved both in water and in phosphate buffer at 75 μM concentration was performed (**Fig. S2**), in order to compare its behaviour in solution with that of the platinum complexes. The UV-vis spectra of *TioxAla* solutions in pure H_2O and PBS (phosphate buffer saline) showed an intense band centred at 256 nm and a marked shoulder at 296 nm (**Fig. S2**). The UV signal, monitored for 72 h, showed no significant changes over time (**Fig. S2b,c**), thus suggesting a good stability of this compound in aqueous solution.

TioxAla was then reacted with the commercially available platinum salt K_2PtCl_4 to obtain Pt(II) complexes, adopting two different synthetic protocols.

3.2. Synthesis and characterization of *TioxAla*-based Pt(II) complexes

In the first complexation reaction (I), 2 equiv. of *TioxAla* were reacted with 1 equiv. of potassium tetrachloroplatinate in acetone/H_2O, 75:25 (v/v). After 3 h stirring at r.t., the solvent was removed under vacuum and treatment with cold methanol provided a single product, hereafter named **Pt1** (91% yield).
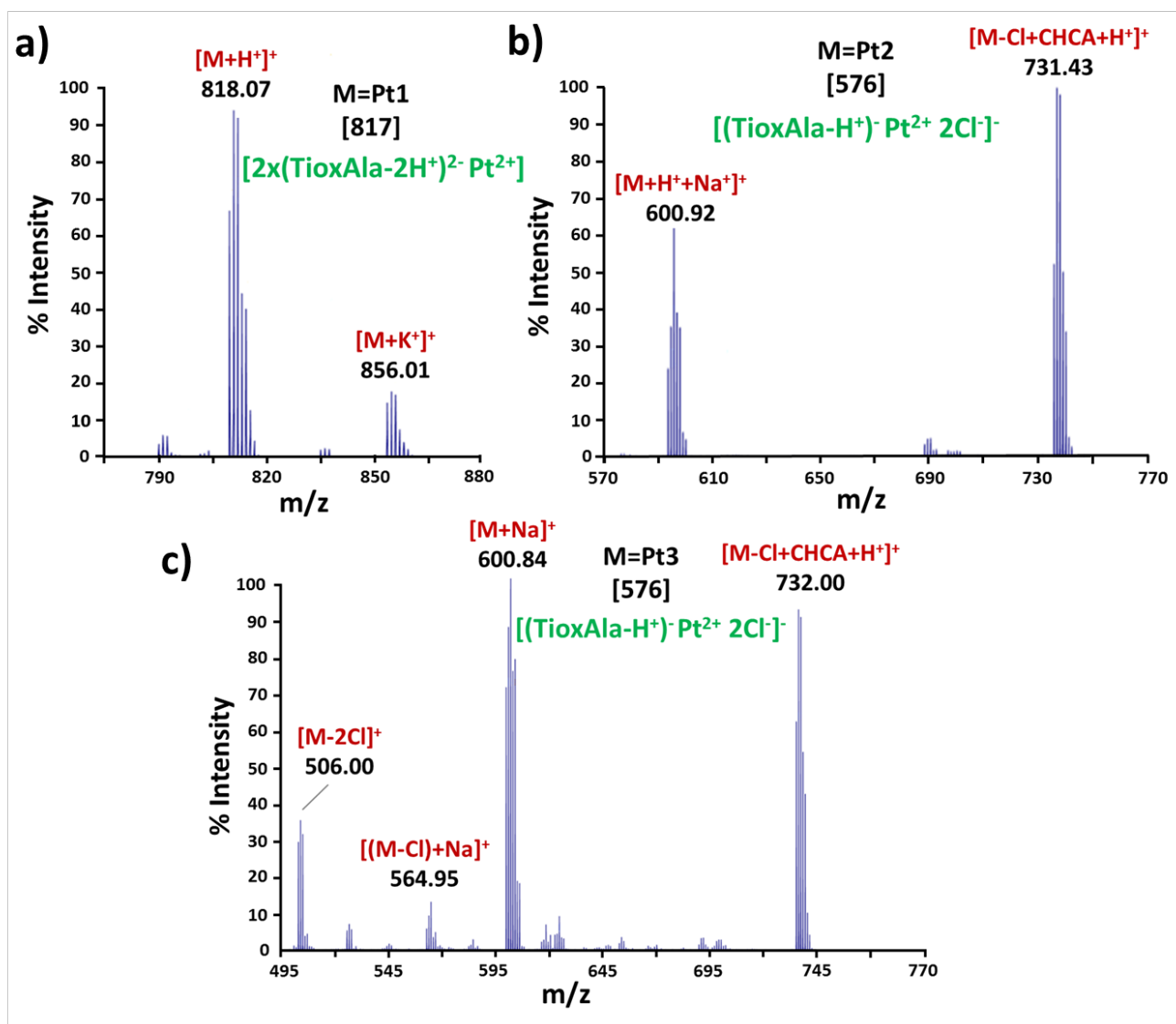
In the second synthetic route (II), *TioxAla* was used as the limiting reagent (0.6 equiv.) with respect to K_2PtCl_4, in the same solvent used for reaction I. After 4 h, the solvent was removed, and from the crude reaction mixture two compounds were obtained with sequential suspensions and centrifugations using acetone first, and then methanol: a more polar compound, named **Pt2**, was recovered from methanol, and another, named **Pt3** was obtained from acetone.

All the Pt complexes were not soluble in water at mM concentration but showed quite good solubility and stability in some organic solvents (such as methanol or acetone). Attempts to obtain crystals of the three complexes suitable for X-ray crystallography were unsuccessful, giving amorphous yellow solids or in some cases degradation products: they were thus characterized by mass spectrometry and NMR spectroscopy.

The MALDI-TOF mass spectrum of **Pt1** showed an intense peak at 818 m/z, corresponding to a molecular formula accounting for a single platinum atom coordinated with two units of *TioxAla* (**Fig. 2a**), together with the peak relative to the potassium ion adduct (M+K$^+$: 856 m/z). The HR ESI-MS spectrum of **Pt1**, reported in **Fig. S4**, also confirmed the molecular formula obtained by MALDI MS data.

The MALDI-TOF mass spectra of **Pt2** and **Pt3** evidenced peaks corresponding to structures consisting of one *TioxAla* unit, one platinum ion and two chloride ions (expected mass for M = 576 Da). Experimentally, for both **Pt2** and **Pt3**, the presence of two main peaks attributable to the monocharged adducts with Na$^+$ (600.92 and 600.84 m/z, for **Pt2** and **Pt3**, respectively) or with the CHCA matrix replacing one chloride ion (731.43 m/z and 732.00 m/z, for **Pt2** and **Pt3**, respectively) were observed (**Fig. 2b,c**). Few weak peaks were also evidenced in the **Pt3** mass spectrum, corresponding to species having lost one (M-Cl+Na$^+$, 564.95 m/z) or both chloride ions (M-2Cl$^-$, 506.00 m/z) (**Fig. 2c**). The HR ESI-MS spectrum of **Pt2** and **Pt3**, reported in **Figs. S7** and **S9**, also

Figure 2: MALDI-TOF mass spectra (positive ion-mode) of **Pt1** (**a**), **Pt2** (**b**) and **Pt3** (**c**), obtained using CHCA as matrix.

Peaks isotopic distribution for each species in the mass spectra of **Pt1**, **Pt2** and **Pt3** was almost superimposable to the theoretical one calculated with the *Isotope Distribution Calculator* program (http://www.sisweb.com/mstools/isotope.htm) (**Fig. S3**).

^{1}H and ^{13}C as well as COSY and HSQC NMR experiments of the three complexes were useful to specifically identify the atoms of the amino acid *TioxAla* directly involved in the binding to the metal (see **Table S1**). The mono- and bi-dimensional NMR spectra for **Pt1**, **Pt2** and **Pt3** are reported in **Figs. S5**, **S6**, **S8 and S10**, and the structures assigned to the three complexes are depicted in **Fig. 1**.

In particular, an up-field shift from 4.63 to 3.85 ppm of the C*H*-α proton (named H), as well as down-field shifts from 4.93 to 5.19 and from 4.69 to 4.81 ppm, respectively for protons G1 and G2 were observed in the ^{1}H NMR spectrum of **Pt1** compared to that of *TioxAla* (**Table S1** and **Fig. S5**, top); in turn, the shifts of carbons H, G, and especially *C*OOH and *C*=S in the ^{13}C NMR spectrum of **Pt1** (**Table S1** and **Fig. S5**, bottom) were also detected. All the observed shifts, together with the absence

12

of proton signals diagnostic of the NH_2 coordinated to platinum, confirmed the exact position of the platinum ion in the complex, according to the structure of **Pt1** presented in **Fig. 1** in which Pt^{2+} coordinates two *TioxAla* ligands through the oxygen of the α-carboxylic functions and the sulfur atoms of the triazolyl-thione rings.

Pt2 showed NMR signals similar to **Pt1** (**Table S1**, and **Fig. S8**), with an upfield shift from 4.63 to 4.16 ppm for proton H, and downfield shifts from 4.93 to 5.27 and from 4.69 to 4.89 ppm, respectively for protons G1 and G2, in the ^{1}H NMR spectrum of **Pt2** compared to that of *TioxAla*. Shifts of the carbon signals G, H, *C*=S and *C*OOH were observed in the ^{13}C NMR spectrum. The observed shifts as well as the multiplicity of the proton signals (**Table S1**) confirmed the coordination to the platinum ion through the sulfur and oxygen atoms, respectively, of the thione and carboxylic functions in **Pt2**, analogously to **Pt1**.

Also for **Pt3**, the NMR analysis was crucial to unambiguously establish the atoms of *TioxAla* coordinating the platinum ion. In particular, extremely diagnostic were the partially exchangeable proton signals of the NH_2 group appearing between 5 and 6 ppm (**Table S1**, and **Fig. S10**, top), as well as the upfield shift from 4.63 to 4.03 ppm of proton H, the down-field shifts from 4.93 to 5.86 and from 4.69 to 4.81 ppm, respectively for protons G1 and G2, in the ^{1}H NMR spectrum of **Pt3** compared to *TioxAla* (**Table S1**); in turn, shifts of the carbon signals G, H, and *C*OOH (**Table S1**, and **Fig. S10**, bottom) were observed from the comparison of ^{13}C NMR spectra of **Pt3** and *TioxAla*. The proton and carbon shifts together with the proton multiplicity evidenced that the platinum ion in **Pt3** is coordinated through the COOH and NH_2 groups, differently from its isomer **Pt2**.

In addition to the variations of the chemical shift values for selected proton signals in the Pt complexes with respect to the starting amino acid, also the signal multiplicity, or the changes of some coupling constants deriving from the presence of platinum, were diagnostic and useful for the structural assignment (**Fig. S11**). The comparison of the proton signals mainly affected by the Pt presence in the **Pt1-Pt3** complexes with respect to the same signals observed for *TioxAla* were reported in **Fig. S11**.

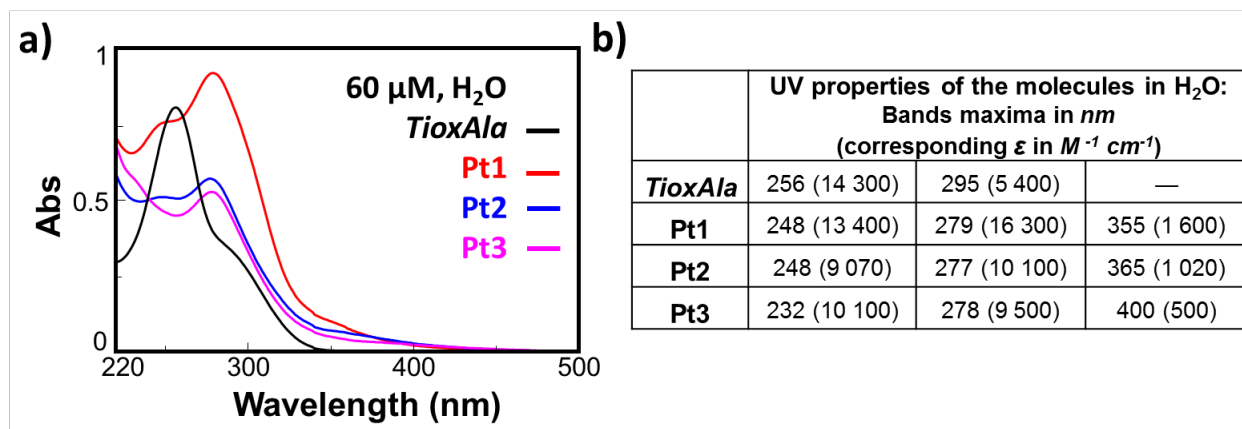## 3.3. UV analysis of the Pt-complexes Pt1, Pt2 and Pt3

A detailed UV analysis of the three complexes was performed recording spectra after their dissolution both in methanol and in aqueous solutions (pure H_2O or PBS), in order to disclose their absorption features and also evaluate possible differences with respect to *TioxAla* due to platinum coordination. Details are reported in the Supporting Information (**Figs. S12-S16**).

In brief, the UV analysis of **Pt1** dissolved in methanol, H_2O or PBS (**Figs. S12** and **S13**) showed that the complex was essentially stable in both the organic solvent and the aqueous solutions, not evidencing shifts of the UV bands over time, generally occurring when chloride ligands are replaced by water molecules in complexes containing Pt-Cl bonds (**Fig. S13e,f**).[35,36] The absence of chloride ligands in **Pt1** was also confirmed by adding, to the platinum complex dissolved in water, $AgNO_3$, able to immediately sequester the chloride ions (details in the SI and in **Fig. S14**).[37]

In contrast, **Pt2** and **Pt3**, stable in CH_3OH, as evidenced by monitoring their UV-vis spectra for 48 h (data not shown), when dissolved either H_2O or in PBS showed an overall reduction of the bands below 300 nm accompanied by shifts of the maxima, with concomitant increase of the band above 350 nm (**Fig. S16a-d**), confirming the presence of exchangeable ligands (chlorides) in both complexes. The presence of exchangeable chloride ligands in the Pt coordination sphere of **Pt2** and

Pt3 was confirmed by treatment of the platinum complexes solutions with an excess of AgNO$_3$, rapidly showing shifts of the UV-bands in their absorption spectra (**Fig. S16e,f**).

A general overview of the absorption features in H$_2$O of the three obtained platinum complexes, in comparison with the starting amino acid, is reported in **Fig. 3**.

a) Overlapped UV-vis spectra with axes Abs (0 to 1) vs Wavelength (nm) (220 to 500), labeled 60 μM, H$_2$O, TioxAla, Pt1, Pt2, Pt3.

b)

	UV properties of the molecules in H$_2$O: Bands maxima in *nm* (corresponding ε in $M^{-1}\,cm^{-1}$)		
TioxAla	256 (14 300)	295 (5 400)	—
Pt1	248 (13 400)	279 (16 300)	355 (1 600)
Pt2	248 (9 070)	277 (10 100)	365 (1 020)
Pt3	232 (10 100)	278 (9 500)	400 (500)

Figure 3: **a**) Overlapped UV-vis spectra of *TioxAla*, **Pt1**, **Pt2** and **Pt3** dissolved in H$_2$O at 60 μM concentration; **b**) Absorption features of the three platinum complexes and the starting amino acid dissolved in H$_2$O. Molar extinction coefficients (ε) were calculated from the slopes of standard calibration curves, constructed using Beer's law.

3.4. Exploring the ability of the new platinum complexes to bind DNA

Subsequently, the three novel Pt(II) complexes were studied in their interaction in solution with DNA using different model systems: 1) two random coil single strands (**ODN1**: CCTCT*GG*TCTCC and **ODN2**: *GG*A*G*ACCA*GA GG*); and 2) two secondary structure-forming oligonucleotides, specifically a 12-base pair duplex (**ODN1/ODN2**) and a unimolecular G-quadruplex (G4, i.e. the tel$_{26}$ sequence[38,39] from the human telomere). Binding experiments were monitored by means of UV-vis and CD spectroscopy in a K$^+$-rich buffered solution (50 mM KCl, 10 mM Na$_2$HPO$_4$/NaH$_2$PO$_4$, pH = 7.2), to mimic the intracellular physiological conditions. All the platinum complexes and the amino acid *TioxAla* did not show any significant contribution to the CD spectra at the concentration used for the experiments; in contrast, the UV contribution of all the compounds was relevant, giving bands overlapping to those the ODNs. However, the use of a two-chambers cell allowed us excluding interferences deriving from the addition of small volumes to the samples, as well as performing in parallel the CD and UV monitoring. In fact, the two-chambers cell permits to record first the *sum* spectrum of the two separated components inserted in the two compartments of the cuvette, and, subsequently – by turning up and down the cell – the spectrum obtained after mixing the solutions (*mix*), registered at different times. Differences between *sum* and *mix* spectra may represent a clear evidence that binding between the platinum complexes and the DNA systems occurs and reflects the corresponding changes in the conformation or stacking of the DNA (mainly monitored by CD), as well as changes in the coordination sphere of Pt (followed by UV). In all the spectroscopic experiments, 4 μM solutions of each DNA system – previously annealed in the K$^+$-rich buffer – were treated with 10 equiv. of each Pt compound, as well as with *TioxAla*. ESI-MS analysis also supported the binding experiments, evidencing if and which platinum adducts are formed. All the ESI-MS experiments were performed incubating the DNA model system (**ODN1** and **ODN2**) with 3 equiv. of each platinum complex and recording spectra after 24 and 48 h. For the preparation and characterization of the structured DNA model systems, see the experimental section and **Fig.**

3.4.1. Investigation of the interaction with the single strand ODNs

No significant difference between the *sum* and *mix* CD spectra relative to the experiments of **ODN1** and **ODN2** with both *TioxAla* and **Pt1** was evidenced (**Fig. S18**), thus indicating no substantial perturbation of the ODNs overall conformation after the treatments. In contrast, after mixing the solutions of **Pt2** and **Pt3** with the single strands, noteworthy changes in the ODN CD spectra were produced (**Fig. 4**), especially for **ODN2**, indicating the formation of significant interactions between the systems accompanied by oligonucleotide conformational changes. In the case of the **ODN2/Pt2** system, an inversion of the positive band of the ODN was even observed (**Fig. 4c**). Probably, the higher reactivity of **Pt2** combined with the higher number of guanines in **ODN2** (6 G *vs* 2 of **ODN1**) were the reasons for this drastic change of the single strand conformation observed already after 2 h.
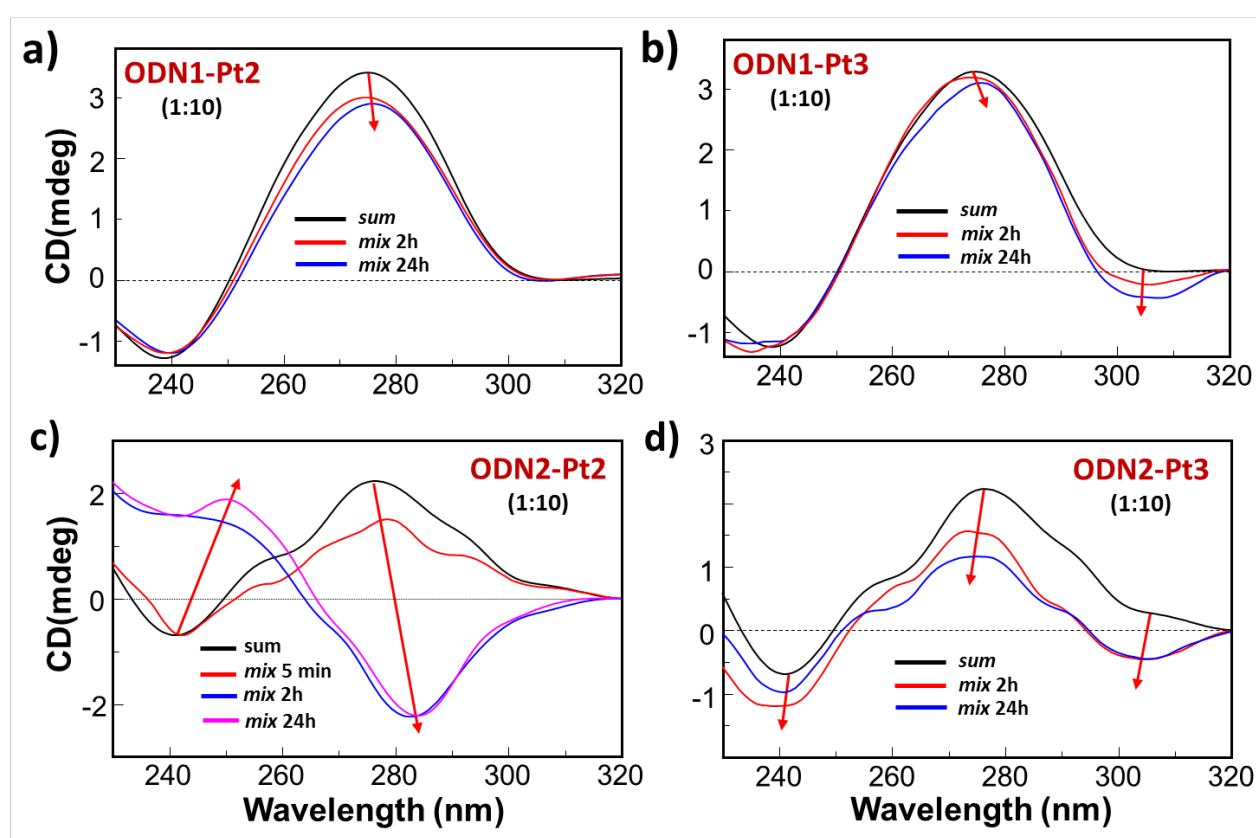

Figure 4: CD-monitored binding experiments with the single stranded random coil ODNs. CD spectra of 4 μM solutions of **ODN1** (**a,b**) or **ODN2** (**c,d**) with 10 equiv. **Pt2** (**a,c**) and **Pt3** (**b,d**), recorded in a two-chambers cell before (*sum*) and after mixing (*mix*) the solutions of the two systems at different times, in 50 mM KCl, 10 mM Na_2HPO_4/NaH_2PO_4, pH = 7.2.

The same solutions used for the CD-binding experiments were analysed also by UV measurements: for all samples, the *mix* spectra showed hyperchromic effects with respect to the corresponding *sum* ones. These effects were more marked for the treatment with **Pt2** and **Pt3**, while only tiny modifications in the absorption profiles were observed with **Pt1** and *TioxAla* (**Fig. S19 and S20**).

To further investigate the ODN/Pt-complex binding interactions, also ESI-MS experiments were performed, incubating the single strands **ODN1** and **ODN2** with 3.0 equiv. of each complex and recording spectra at 24 (**Figs. 5** and **6**, respectively) and 48 h (**Fig. S21** and **S22**), following a well

established protocol.[11,40,41] In **Figs. 5a** and **6a** the ESI-MS spectra of intact **ODN1** and **ODN2**, showing main peaks at, respectively, 3547.037 and 3742.444 Da (corresponding to the molecular peak masses, M), were reported: other peaks were assigned to ODNs sodiated forms (3569.006 and 3591.012 Da, mono- and di-sodiated **ODN1**, respectively; 3764.417 Da mono-sodiated **ODN2**). In line with UV and CD results, the incubation of **ODN1** and **ODN2** with **Pt1** did not afford any significant oligonucleotide-platinum complex adduct (**Figs. 5b** and **6b**), even after 48 h incubation (**Fig. S21a** and **S22a**). On the contrary, the incubation with **Pt2** and **Pt3** complexes produced after 24 h significative adducts between **ODN1** or **ODN2** and mainly the fragment *TioxAla*-Pt (mono and bis-adducts) (**Figs. 5c,d** and **S23** relatively to **ODN1**; **Figs. 6c,d** relatively to **ODN2**), showing that the nucleobases bound the Pt complex replacing both its chloride ions. Although the main and well-documented Pt binding site is represented by the GG motif,[42] the presence of a non-negligible amount of a *TioxAla*-Pt/**ODN1** bis-adduct pointed out to the existence of an alternative binding site. Indeed, secondary binding sites have been described in the scientific literature, such as the CC motif present in **ODN1**.[43–45] Moreover, as observed in **Figs. S21b,c** and **S22b,c**, the peaks relative to these species had a reduced intensity in the ESI spectra recorded after 48 h incubation time with a concomitant decrease of the signal/noise ratio, indicating an evolution of these and other less intense adducts towards other species. This effect could be probably due to the excess of the complexes with respect to the DNA, responsible for the metallation of a secondary site. Also, similar effects might be determined by the instability of the adducts and their consequent rearrangement. Interestingly, a higher reactivity was evidenced for **Pt2** with respect to **Pt3** in the interaction with the single strands, in accordance with the behaviour observed by spectroscopic measurements.
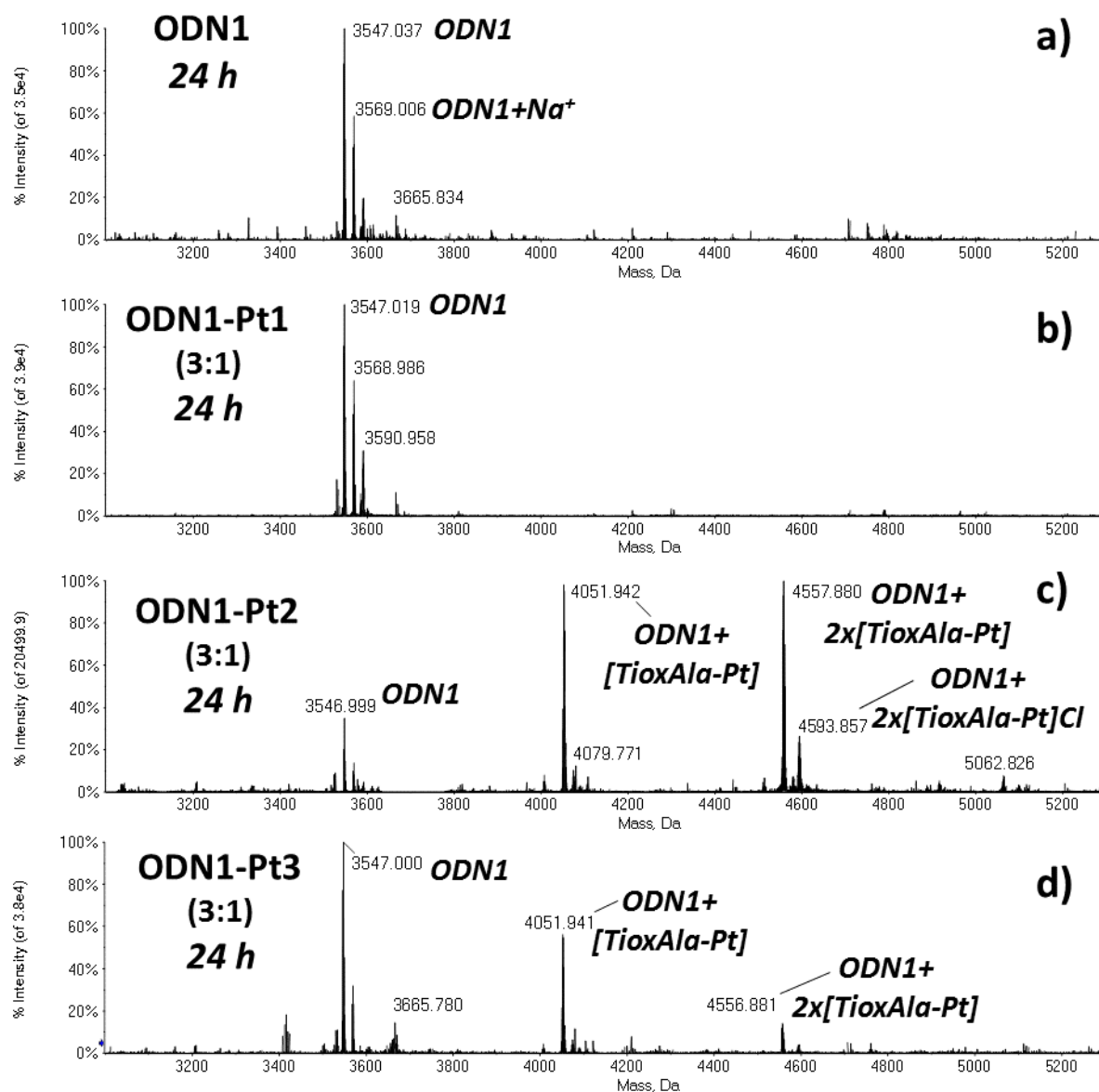
Figure 5: Deconvoluted ESI mass spectra of **ODN1** (6 µM solution) in water (**a**) and incubated at 37 °C for 24 h with **Pt1** (**b**), **Pt2** (**c**), and **Pt3** (**d**) at 3:1 metal to ODN molar ratio.
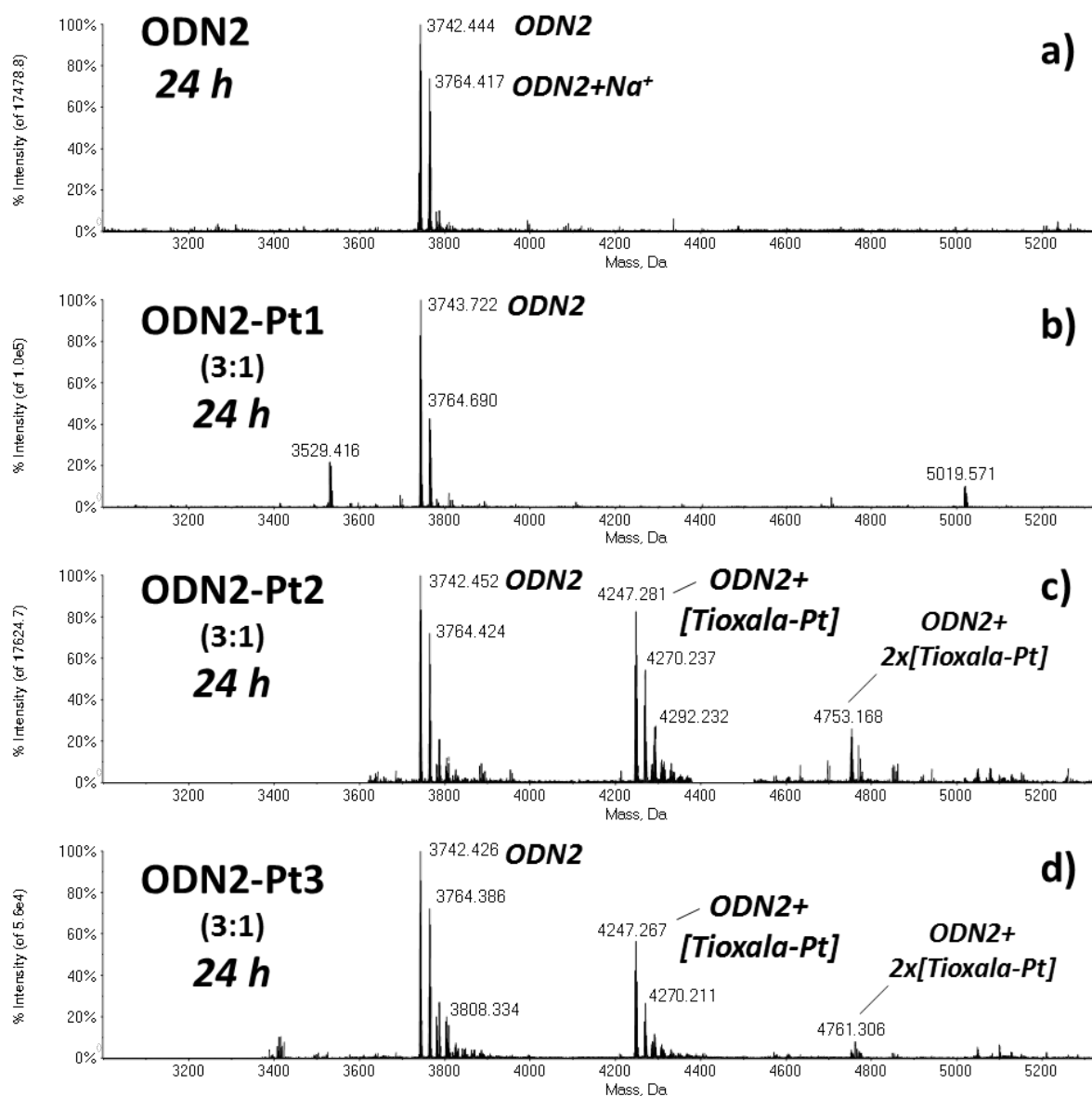
Figure 6: Deconvoluted ESI mass spectra of **ODN2** (6 µM solution) in water (**a**) and incubated at 37 °C for 24 h with **Pt1** (**b**), **Pt2** (**c**), and **Pt3** (**d**) at 3:1 metal to ODN molar ratio.

3.4.2. Investigation of the interaction with the structured DNA: duplex and G-quadruplex model systems

The interaction between the novel platinum complexes, using *TioxAla* as control, and the DNA duplex (formed by mixing equimolar amounts of **ODN1** and **ODN2**, as described in the experimental section) was also investigated by CD and UV spectroscopy.

As observed in the experiments with the single strand oligonucleotides, also for the duplex the highest conformational changes, monitored by CD, were evidenced for **Pt2** (**Fig. S24**), with the general reactivity order: **Pt2** > **Pt3** > **Pt1** ≈ *TioxAla*.

Regarding the UV experiments, as for **ODN1** and **ODN2**, after mixing the duplex with the various platinum compounds in the two-chambers cell, the absorption spectra significantly increased (**Fig. S25**). Once again, this effect was more pronounced for **Pt2**, whose interaction with the duplex gave a drastic increase in the UV signal at 260 nm compared to the other compounds.

The interaction of the new Pt(II) complexes and *TioxAla* with the G4-forming tel$_{26}$ was also investigated. In the case of *TioxAla* and **Pt1**, slight conformational changes of the G4 were evidenced by CD spectra, showing a decrease of the 289 nm band with concomitant increase, more marked for **Pt1**, of the CD signal at 267 nm (**Fig. 7a,b**). The treatment of the G4 with **Pt2** and **Pt3** induced remarkable conformational changes of the oligonucleotide structure, especially in the case of **Pt2**, reflected in this case also in significant shifts of the maxima of the 290- and, mainly, 267-nm bands (**Fig. 7c,d**).
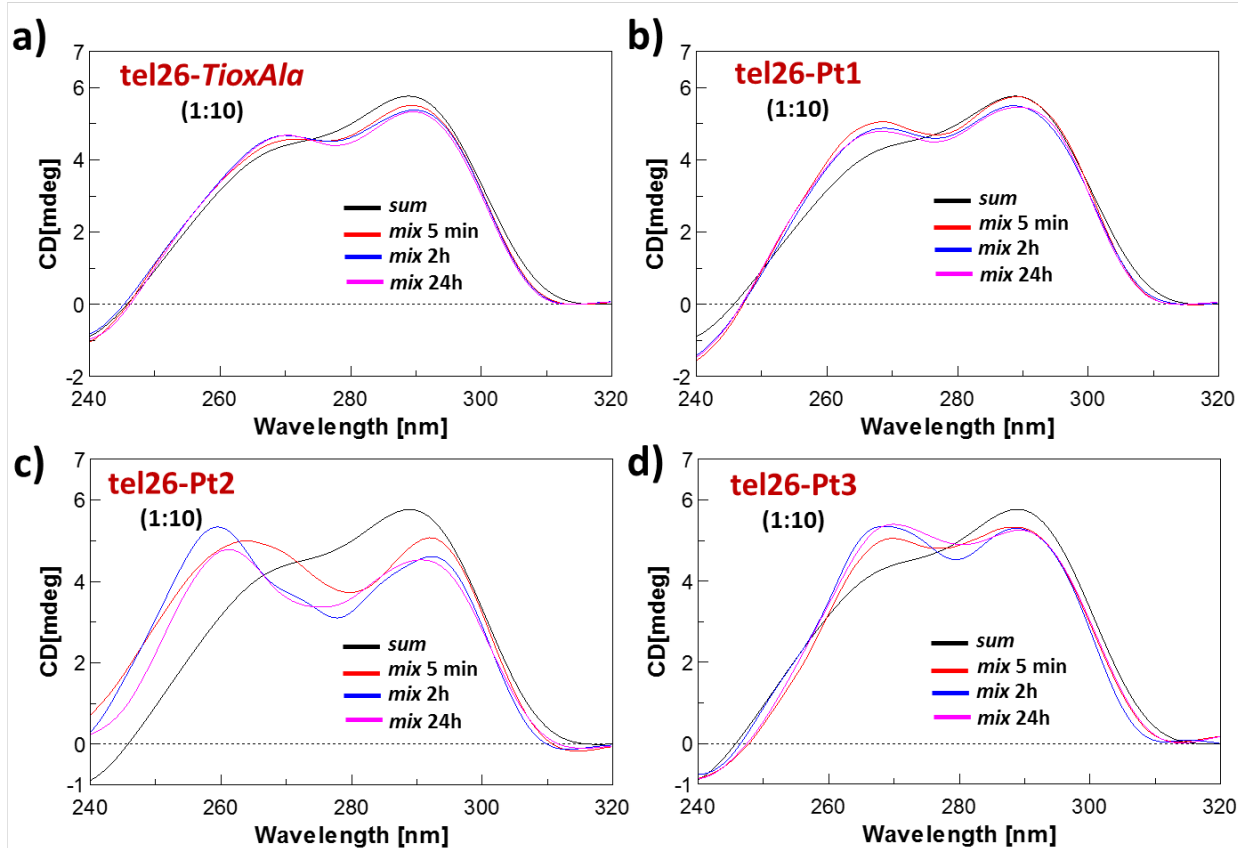

Figure 7: CD-monitored binding experiments with the G-quadruplex DNA. CD spectra of tel$_{26}$ G4 (4 µM) and the various compounds (10 equiv. each), *TioxAla* (**a**), **Pt1** (**b**), **Pt2** (c) and **Pt3** (**d**), recorded in a two-chambers cell before (*sum*) and after mixing (*mix*) the solutions of the two systems at different times, in 50 mM KCl, 10 mM Na$_2$HPO$_4$/NaH$_2$PO$_4$, pH = 7.2.

The interaction of *TioxAla*, **Pt1**, **Pt2** and **Pt3** with tel$_{26}$ was also evaluated by UV-vis analysis: with *TioxAla*, the resulting solution gave a slight hypochromic effect (**Fig. S26a**); in the case of **Pt1**/G4, after mixing the solutions, no significant difference between the *mix* and *sum* spectra was observed (**Fig. S26b**), whereas with **Pt2** and **Pt3** significant hyperchromic effects were evidenced (**Fig. S26c,d**). In particular, the *mix* UV spectrum of the G4 with **Pt3** evolved over time affording, after 1 h, the collapse of the 255- and 281-nm bands in a single, enlarged band, with absorption maximum at 276 nm.

3.5. Antiproliferative activity of the novel Pt(II)-based complexes

In order to evaluate the effects of **Pt1**, **Pt2** and **Pt3** on cell proliferation, preliminary MTT assays were performed on two human cancer cell lines (HeLa, from cervix adenocarcinoma, and A375, from malignant melanoma) and on normal cells (HDF, human dermal fibroblasts). The selected cell lines

were incubated with the three platinum complexes or the starting amino acid *TioxAla*, used as reference, for 48 h. Cisplatin and the vehicle were respectively used as positive and negative controls. The results indicated that *TioxAla* and **Pt1** was essentially not active on cancer cell lines, whereas **Pt2** and **Pt3** inhibited the proliferation of the cancer cells A375 of about 40% at 48 h (**Fig. 8**). Differently from **Pt3**, **Pt2** was also active, even if in less degree (about 20% proliferation inhibition at 48 h), on HeLa cells (**Fig. 8**). In all the experiments, the effects of the tested Pt(II)-complexes is lower than those produced by cisplatin, but more selective: indeed, contrarily to cisplatin, **Pt2** and **Pt3** did not affect normal fibroblasts (**Fig. 8**). The results of **Pt1** could be rationalized on the basis of its structure and in particular on the absence of chlorides as chelating ligands for the metal centre, which make the complex more stable to nucleophilic attack by biomolecule targets.
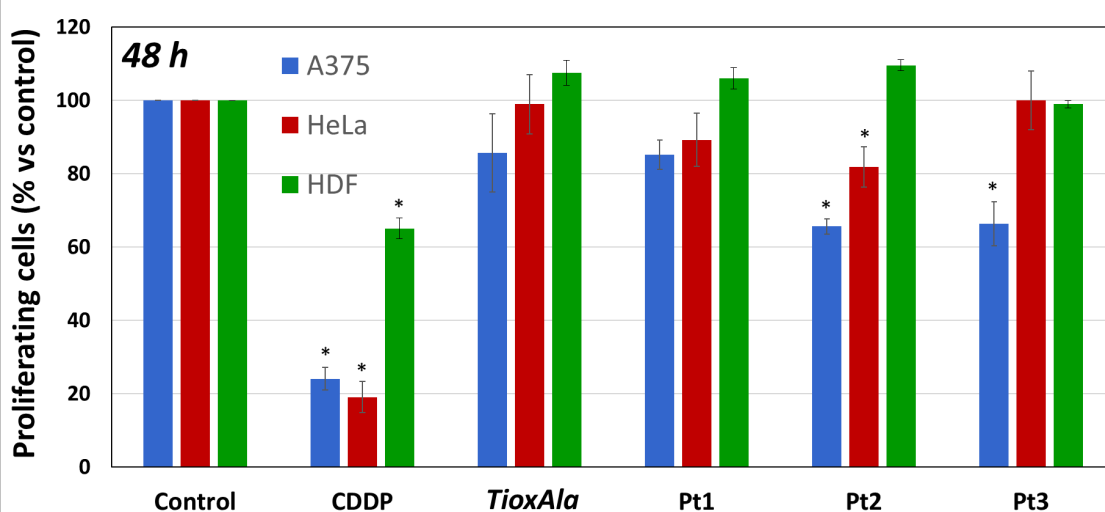

Figure 8: Cells were incubated with 50 µM Pt(II) complexes, *TioxAla* or 10 µM CDDP for 48 h. The results are presented as percentage of proliferating cells with respect to the control (vehicle treated cells) and are expressed as means ± SE of three independent experiments (* $p < 0.05$).

Furthermore, a deeper characterization, consisting in IC$_{50}$ values calculation, on the most sensitive cancer cell line (A375 cells) was performed on the most active compounds, **Pt2** and **Pt3**. The results showed an IC$_{50}$ value of 80.0 µM (R^2 = 99.0%) for **Pt2** and >100 µM for **Pt3**, both higher than that observed for cisplatin (1.36 µM).

3.6. Exploring the antiproliferative mechanism for the new platinum complexes: annexin V binding assay

In order to establish if cellular death caused by the new Pt complexes was due to apoptosis or necrosis processes, the annexin V-FITC assay was carried out by cytofluorimetric assays (see SI for details). In particular, the assay was performed on the cancer cell line found most sensitive to Pt complexes. A375 cells were thus treated with **Pt2** (the most active compound), and, 48 h after treatment, no increase in early or late apoptosis cell amounts was observed (low and upper right quadrants, **Fig. 9**), thus indicating that the complex did not induce apoptosis but necrosis, also in line with the behaviour showed by other platinum-based complexes.[46]
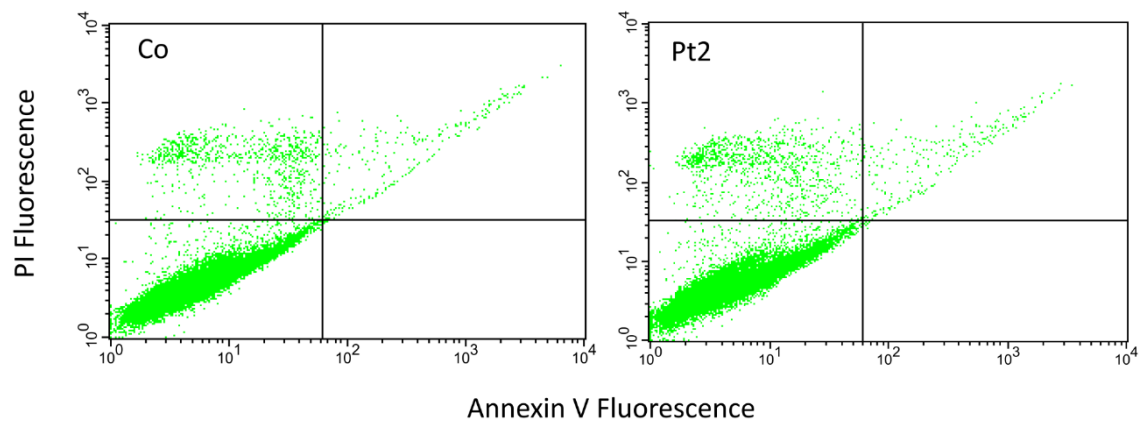
Figure 9: Apoptosis analyses with annexin V-FITC/PI double staining on A375 cells. Untreated cells (Co); **Pt2** treated cells (Pt2); Upper left quadrant: necrotic cells; upper right: advanced apoptotic cells; lower left: viable cells; lower right: early apoptotic cells. These pictures are representative of three independent experiments.

4. Conclusions

In the search for novel cisplatin-like complexes, we here selected an RNA-binding amino acid based on L-alanine, with a triazolyl-thione group on the side chain, named *TioxAla,* previously synthesized by some of us, as a valuable scaffold for the preparation of new platinum complexes. In this design, a synergic activity was expected, owing to the concomitant presence of the platinum ion and the bioactive amino acid.

Thus, the complexation reaction of *TioxAla* with K_2PtCl_4 was performed, using both an excess (2 equiv., reaction I) or a defect (0.6 equiv., reaction II) of the amino acid with respect to the Pt(II) salt. Three new platinum complexes were isolated: a compound consisting of two amino acid units coordinating one Pt(II) ion, named **Pt1** (from reaction I), and two isomers, **Pt2** and **Pt3**, including one *TioxAla* unit, one platinum ion and two chloride ligands. The molecular structures of the three complexes were definitively assessed by a combined approach of mass spectrometry (MALDI-TOF MS, HR ESI-MS) and mono- and bidimensional NMR spectroscopy techniques. **Pt1** and **Pt2** coordinated the platinum ion through the sulfur atom of the thione group and the carboxylate function, whereas **Pt3** exploited the α-amino and carboxylic functions.

UV-vis spectroscopic analysis evidenced good stability over time in organic solvents (such as methanol or acetone) for all the complexes, with hydrolysis events occurring only for **Pt2** and **Pt3** in aqueous solutions, where the chloride ions were exchanged with water molecules.

In order to explore the ability of the new platinum complexes to bind DNA, **Pt1**, **Pt2**, **Pt3**, as well as *TioxAla* as reference, were studied in solution in their interaction with different DNA model systems, including two random coil single strands, a duplex and a G-quadruplex structure, using UV-vis and CD spectroscopies along with ESI mass spectrometry. Taken together, all the binding studies evidenced that: 1) **Pt1** was not able to establish coordinative bonds with the single strand oligonucleotides, as expected for the lack of exchangeable chloride ions; 2) both **Pt2** and **Pt3** were able to form well-defined adducts with the single strand ODNs, mainly mono and bis-adducts between the ODNs and the fragment *TioxAla*-Pt (as evidenced by ESI-MS experiments), indicating that the nucleobases bound platinum replacing the chloride ions; 3) **Pt2** and **Pt3** produced conformational changes more dramatic on **ODN2** than on **ODN1**, as evidenced by CD experiments, in line with the guanine content (6 G in **ODN2** *vs* 2 in **ODN1**); 4) both the duplex **ODN1**/**ODN2** and the well-packed guanine residues of the G-quadruplex structure of the tel_{26} were bound by **Pt2** and **Pt3** but not **Pt1**; 5) no substantial perturbation of the DNA overall conformation was observed after treatment with *TioxAla* ligand.

Furthermore, preliminary antiproliferative assays of the complexes were performed on two cancer cells (HeLa and A375) as well as on a normal cell line (HDF). The results indicated that *TioxAla* and **Pt1** were essentially not active on cancer cell lines, whereas **Pt2** and **Pt3** evidenced moderate cytotoxicity inhibiting the proliferation of the A375 cancer cells of about 40% at 48 h. In all the experiments, the cytotoxicity of Pt(II)-complexes was lower than that of cisplatin, used as positive control, but more selective towards tumour cells with respect to normal cells: indeed, contrarily to cisplatin, **Pt2** and **Pt3** did not affect normal fibroblasts. Annexin V-FITC assay established that the most active compound (**Pt2**) did not induce apoptosis but necrosis on the most sensitive cancer cell line (A375).

Taken together, all the reported data demonstrate that the bioactivity of the complexes, even if weak, seems to be connected to the DNA binding ability, which is in turn related to the presence of chlorides ligands coordinating Pt(II) ion in the structure of the complexes. Indeed, while *TioxAla* and the

chloride-free complex **Pt1**, were not able to bind DNA in solution and were found not bioactive, the chloride-containing complexes **Pt2** and **Pt3** exhibited marked interactions with DNA and proved to be cytotoxic.

Given the high propensity of **Pt2** and **Pt3** to bind and distort DNA structures, we hypothesize that the scarce in vitro bioactivity could be due to deactivation processes occurring in the extracellular environments before that Pt(II)-complexes can reach their specific intracellular target. These deactivation/hydrolysis phenomena could be ascribed to the binding with serum proteins or to a not-efficient cell uptake, ultimately reducing the active amount of the drug able to exert its biological activity. Thus, in future efforts we will synthesize other derivatives of **Pt2** and **Pt3** possibly with greater stability in aqueous media (for example substituting one of the chloride ligands with a DMSO molecule, etc.) to prevent their partial deactivation. In alternative, also the use of supramolecular systems (such as liposomes or nanoparticles) can be exploited to efficiently protect the here investigated Pt(II)-complexes enhancing the active amount to be internalized by the cells.[47,48]

Finally, more in-depth biological assays will be also carried out extending the analysis to other human cancer cells in order to found potential cell lines sensitive to the new complexes.

Abbreviation

A375 (human melanoma cells); CD (circular dichroism); CDDP (cisplatin); CHCA (α-cyano-hydroxycinnamic acid); DAPA (diaminopropanoic acid); DHB (2,5-dihydroxybenzoic acid); DMEM (Dulbecco's Modified Eagle's Medium); DMSO (dimethyl sulfoxide); ESI (electrospray ionization); FBS (fetal bovine serum); FITC (fluorescein isothiocyanate); HDF (human dermal fibroblast); HeLa (human cervix adenocarcinoma cells); HR (high resolution); IC$_{50}$ (50% inhibitory concentration); LC (liquid chromatography); MALDI (matrix assisted laser desorption ionization); MS (mass spectrometry); MTT [3-(4,5-dimethylthiazol-2-yl)-2,5-diphenyltetrazolium bromide]; NMR (nuclear magnetic resonance); ODN (oligodeoxyribonucleotides); PBS (phosphate buffer saline); SE (standard error); SI (supporting information); THAP (2,4,6-trihydroxyacetophenone); TLC (thin layer chromatography); TOF (time of flight); UV (ultraviolet); vis (visible).

Acknowledgements

References:

[1]   L. Kelland, The resurgence of platinum-based cancer chemotherapy, Nat. Rev. Cancer. 7 (2007) 573–584. doi:10.1038/nrc2167.

[2]   S. Dasari, P. Bernard Tchounwou, Cisplatin in cancer therapy: molecular mechanisms of action, Eur. J. Pharmacol. 740 (2014) 364–378. doi:10.1016/j.ejphar.2014.07.025.

[3]   V. Brabec, J. Kasparkova, Modifications of DNA by platinum complexes: relation to resistance of tumors to platinum antitumor drugs, Drug Resist. Updat. 8 (2005) 131–146. doi:10.1016/j.drup.2005.04.006.

[4]   D. Musumeci, C. Platella, C. Riccardi, A. Merlino, T. Marzo, L. Massai, L. Messori, D. Montesarchio, A first-in-class and a fished out anticancer platinum compound: cis-[PtCl$_2$(NH$_3$)$_2$] and cis-[PtI$_2$(NH$_3$)$_2$] compared for their reactivity towards DNA model systems, Dalton Trans. 45 (2016) 8587–8600. doi:10.1039/C6DT00294C.

[5]   M.S. Davies, S.J. Berners-Price, T.W. Hambley, Slowing of cisplatin aquation in the presence of DNA but not in the presence of phosphate: improved understanding of sequence selectivity and the roles of monoaquated and diaquated species in the binding of cisplatin to DNA, Inorg. Chem. 39 (2000) 5603–5613. doi:10.1021/ic000847w.

[6]   J.J. Wilson, S.J. Lippard, Synthetic methods for the preparation of platinum anticancer complexes, Chem. Rev. 114 (2014) 4470–4495. doi:10.1021/cr4004314.

[7]   M. Van Beusichem, N. Farrell, Activation of the trans geometry in platinum antitumor complexes. Synthesis, characterization, and biological activity of complexes with the planar ligands pyridine, N-methylimidazole, thiazole, and quinoline. Crystal and molecular structure of trans-dichlorobis(thiazole)platinum(II), Inorg. Chem. 31 (1992) 634–639. doi:10.1021/ic00030a021.

[8]   F.J. Ramos-Lima, O. Vrána, A.G. Quiroga, C. Navarro-Ranninger, A. Halámiková, H. Rybníčková, L. Hejmalová, V. Brabec, Structural characterization, DNA interactions, and cytotoxicity of new transplatin analogues containing one aliphatic and one planar heterocyclic

amine ligand, J. Med. Chem. 49 (2006) 2640–2651. doi:10.1021/jm0602514.

[9]   S. Roy, J.A. Westmaas, F. Buda, J. Reedijk, Platinum(II) compounds with chelating ligands based on pyridine and pyrimidine: synthesis, characterizations, DFT calculations, cytotoxic assays and binding to a DNA model base, J. Inorg. Biochem. 103 (2009) 1278–1287. doi:10.1016/j.jinorgbio.2009.07.004.

[10] F. Gümüş, G. Eren, L. Açik, A. Çelebi, F. Öztürk, Ş. Yilmaz, R.I. Sağkan, S. Gür, A. Özkul, A. Elmali, Y. Elerman, Synthesis, cytotoxicity, and DNA interactions of new cisplatin analogues containing substituted benzimidazole ligands, J. Med. Chem. 52 (2009) 1345–1357. doi:10.1021/jm8000983.

[11] L. Massai, A. Pratesi, J. Bogojeski, M. Banchini, S. Pillozzi, L. Messori, Ž.D. Bugarčić, Antiproliferative properties and biomolecular interactions of three Pd(II) and Pt(II) complexes, J Inorg Biochem. 165 (2016) 1–6.

[12] E. Budzisz, U. Krajewska, M. Rozalski, A. Szulawska, M. Czyz, B. Nawrot, Biological evaluation of novel Pt(II) and Pd(II) complexes with pyrazole-containing ligands, Eur. J. Pharmacol. 502 (2004) 59–65. doi:10.1016/j.ejphar.2004.08.053.

[13] F.K. Keter, S. Kanyanda, S.S.L. Lyantagaye, J. Darkwa, D.J.G. Rees, M. Meyer, In vitro evaluation of dichloro-bis(pyrazole)palladium(II) and dichloro-bis(pyrazole)platinum(II) complexes as anticancer agents, Cancer Chemother. Pharmacol. 63 (2008) 127–138. doi:10.1007/s00280-008-0721-y.

[14] T. V. Serebryanskaya, T. Yung, A.A. Bogdanov, A. Shchebet, S.A. Johnsen, A.S. Lyakhov, L.S. Ivashkevich, Z.A. Ibrahimava, T.S. Garbuzenco, T.S. Kolesnikova, N.I. Melnova, P.N. Gaponik, O.A. Ivashkevich, Synthesis, characterization, and biological evaluation of new tetrazole-based platinum(II) and palladium(II) chlorido complexes - Potent cisplatin analogues and their trans isomers, J. Inorg. Biochem. 120 (2013) 44–53. doi:10.1016/j.jinorgbio.2012.12.001.

[15] A. Muscella, N. Calabriso, S.A. De Pascali, L. Urso, A. Ciccarese, F.P. Fanizzi, D. Migoni, S.

Marsigliante, New platinum(II) complexes containing both an O,O′-chelated acetylacetonate ligand and a sulfur ligand in the platinum coordination sphere induce apoptosis in HeLa cervical carcinoma cells, Biochem. Pharmacol. 74 (2007) 28–40. doi:10.1016/j.bcp.2007.03.027.

[16] C. Mügge, R. Liu, H. Görls, C. Gabbiani, E. Michelucci, N. Rüdiger, J.H. Clement, L. Messori, W. Weigand, Novel platinum(II) compounds with O,S bidentate ligands: synthesis, characterization, antiproliferative properties and biomolecular interactions, Dalton Trans. 43 (2014) 3072–3086. doi:10.1039/c3dt52284a.

[17] C. Mügge, T. Marzo, L. Massai, J. Hildebrandt, G. Ferraro, P. Rivera-Fuentes, N. Metzler-Nolte, A. Merlino, L. Messori, W. Weigand, Platinum(II) complexes with O,S bidentate ligands: biophysical characterization, antiproliferative activity, and crystallographic evidence of protein binding, Inorg. Chem. 54 (2015) 8560–8570. doi:10.1021/acs.inorgchem.5b01238.

[18] C. Mügge, D. Musumeci, E. Michelucci, F. Porru, T. Marzo, L. Massai, L. Messori, W. Weigand, D. Montesarchio, Elucidating the reactivity of Pt(II) complexes with (O,S) bidentate ligands towards DNA model systems, J. Inorg. Biochem. 160 (2016) 198–209. doi:10.1016/j.jinorgbio.2016.02.013.

[19] A. Iakovidis, N. Hadjiliadis, Complex compounds of platinum (II) and (IV) with amino acids, peptides and their derivatives, Coord. Chem. Rev. 135–136 (1994) 17–63. doi:10.1016/0010-8545(94)80064-2.

[20] J. Altman, M. Wilchek, Platinum(II) complexes with diaminopropionic acid as oxygen-bound unidentate, nitrogen-oxygen and nitrogen-2nitrogen chelate complexes, Inorganica Chim. Acta. 101 (1985) 171–173. doi:10.1016/S0020-1693(00)87651-3.

[21] S. Moradell, J. Lorenzo, A. Rovira, M.S. Robillard, F.X. Avilés, V. Moreno, R. De Llorens, M.A. Martinez, J. Reedijk, A. Llobet, Platinum complexes of diaminocarboxylic acids and their ethyl ester derivatives: the effect of the chelate ring size on antitumor activity and interactions with GMP and DNA, J. Inorg. Biochem. 96 (2003) 493–502. doi:10.1016/S0162-

0134(03)00252-6.

[22]   S. D'Errico, N. Borbone, V. Piccialli, E. Di Gennaro, A. Zotti, A. Budillon, C. Vitagliano, I. Piccialli, G. Oliviero, Synthesis and evaluation of the antitumor properties of a small collection of PtII complexes with 7-deazaadenosine as scaffold, Eur. J. Org. Chem. 2017 (2017) 4935–4947. doi:10.1002/ejoc.201700730.

[23]   A.S. Saghyan, H.M. Simonyan, S.G. Petrosyan, A. V. Geolchanyan, G.N. Roviello, D. Musumeci, V. Roviello, Thiophenyl-substituted triazolyl-thione l-alanine: asymmetric synthesis, aggregation and biological properties, Amino Acids. 46 (2014) 2325–2332. doi:10.1007/s00726-014-1782-3.

[24]   G.N. Roviello, D. Musumeci, Synthetic approaches to nucleopeptides containing all four nucleobases, and nucleic acid-binding studies on a mixed-sequence nucleo-oligolysine, RSC Adv. 6 (2016) 63578–63585. doi:10.1039/c6ra08765e.

[25]   G.N. Roviello, C. Vicidomini, S. Di Gaetano, D. Capasso, D. Musumeci, V. Roviello, Solid phase synthesis and RNA-binding activity of an arginine-containing nucleopeptide, RSC Adv. 6 (2016) 14140–14148. doi:10.1039/c5ra25809j.

[26]   B. Damnjanović, B. Petrović, J. Dimitrić-Marković, M. Petković, Comparison of MALDI-TOF mass spectra of [PdCl(dien)]Cl and [Ru(en)$_2$Cl$_2$]Cl acquired with different matrices, J. Serbian Chem. Soc. 76 (2011) 1687–1701. doi:10.2298/JSC110201145D.

[27]   D. Musumeci, G.N. Roviello, G. Rigione, D. Capasso, S. Di Gaetano, C. Riccardi, V. Roviello, D. Montesarchio, Benzodifuran derivatives as potential antiproliferative agents: possible correlation between their bioactivity and aggregation properties, Chempluschem. 82 (2017) 251–260. doi:10.1002/cplu.201600547.

[28]   C. Platella, S. Guida, L. Bonmassar, A. Aquino, E. Bonmassar, G. Ravagnan, D. Montesarchio, G.N. Roviello, D. Musumeci, M.P. Fuggetta, Antitumour activity of resveratrol on human melanoma cells: a possible mechanism related to its interaction with malignant cell telomerase, Biochim.   Biophys.   Acta - Gen.   Subj.   1861   (2017)   2843–2851.

doi:10.1016/j.bbagen.2017.08.001.

[29] J. Amato, C. Platella, S. Iachettini, P. Zizza, D. Musumeci, S. Cosconati, A. Pagano, E. Novellino, A. Biroccio, A. Randazzo, B. Pagano, D. Montesarchio, Tailoring a lead-like compound targeting multiple G-quadruplex structures, Eur J Med Chem. 1 (2019) 163:295-306. doi:10.1016/j.ejmech.2018.11.058.

[30] G.N. Roviello, S. Di Gaetano, D. Capasso, A. Cesarani, E.M. Bucci, C. Pedone, Synthesis, spectroscopic studies and biological activity of a novel nucleopeptide with Moloney murine leukemia virus reverse transcriptase inhibitory activity, Amino Acids. 38 (2010) 1489–1496. doi:10.1007/s00726-009-0361-5.

[31] M. Adinolfi, D. Capasso, S. Di Gaetano, A. Iadonisi, L. Leone, A. Pastore, A straightforward synthetic access to symmetrical glycosyl disulfides and biological evaluation thereof, Org. Biomol. Chem. 9 (2011) 6278–6283. doi:10.1039/c1ob05619k.

[32] J. Amato, A. Pagano, D. Capasso, S. Di Gaetano, M. Giustiniano, E. Novellino, A. Randazzo, B. Pagano, Targeting the BCL2 gene promoter G-Quadruplex with a new class of furopyridazinone-based molecules, ChemMedChem. 13 (2018) 406–410. doi:10.1002/cmdc.201700749.

[33] D. Capasso, I. De Paola, A. Liguoro, A. Del Gatto, S. Di Gaetano, D. Guarnieri, M. Saviano, L. Zaccaro, RGDechi-hCit: αvβ3 selective pro-apoptotic peptide as potential carrier for drug delivery into melanoma metastatic cells, PLoS One. 9 (2014) e106441. doi:10.1371/journal.pone.0106441.

[34] D. Capasso, S. Di Gaetano, V. Celentano, D. Diana, L. Festa, R. Di Stasi, L. De Rosa, R. Fattorusso, L.D. D'Andrea, Unveiling a VEGF-mimetic peptide sequence in the IQGAP1 protein, Mol. Biosyst. 13 (2017) 1619–1629. doi:10.1039/c7mb00190h.

[35] D. Musumeci, L. Rozza, A. Merlino, L. Paduano, T. Marzo, L. Massai, L. Messori, D. Montesarchio, Interaction of anticancer Ru(III) complexes with single stranded and duplex DNA model systems, Dalton Trans. 44 (2015) 13914–13925. doi:10.1039/c5dt01105a.
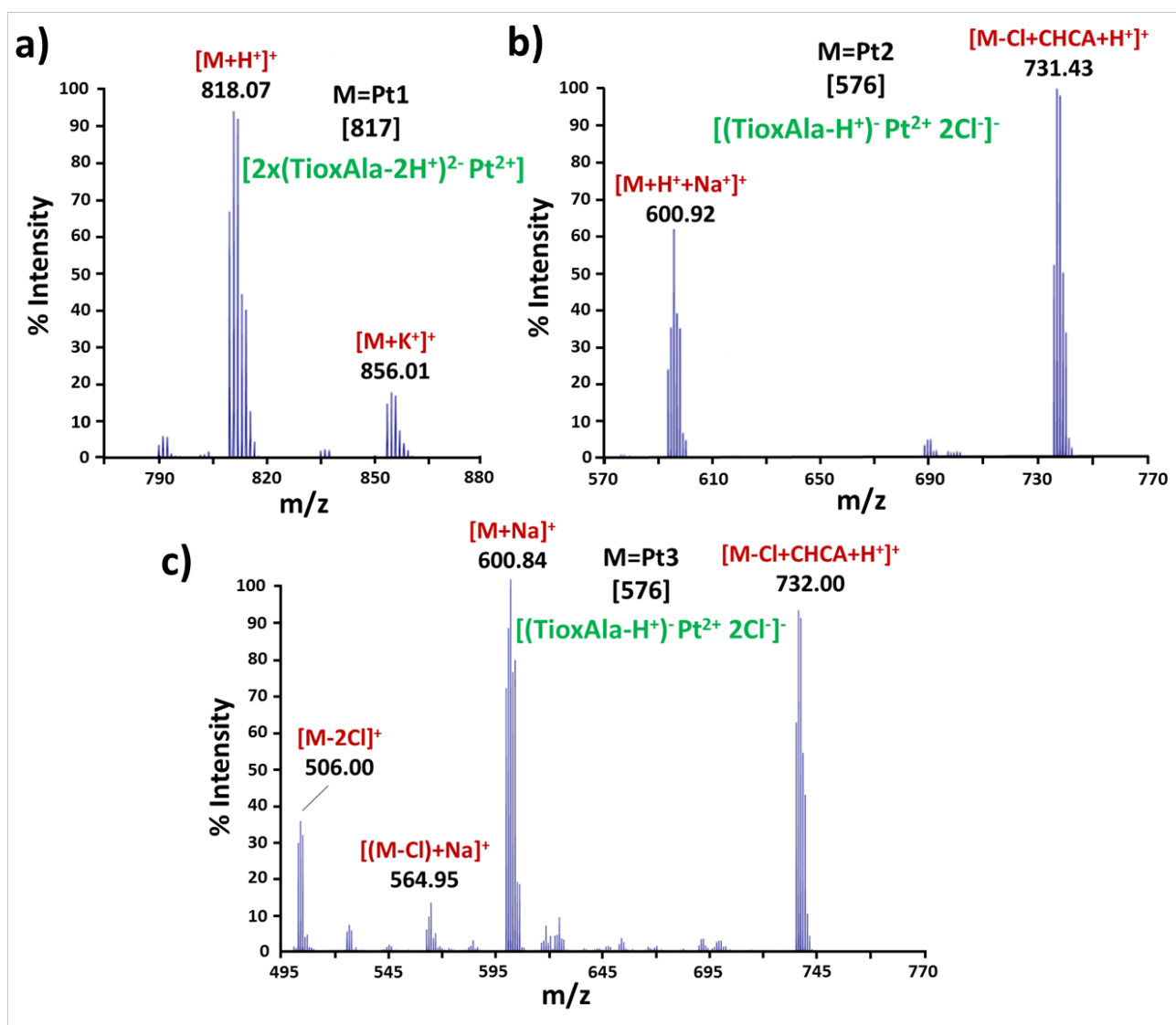
[36] H. Terraschke, M. Rothe, P. Lindenberg, In situ monitoring metal-ligand exchange processes by optical spectroscopy and X-ray diffraction analysis: a review, Rev. Anal. Chem. 37 (2018) 20170003. doi:10.1515/revac-2017-0003.

[37] C.H. Greene, L.D. Frizzell, Studies of the precipitation of silver chloride II from silver nitrate and hydrochloric acid, J. Am. Chem. Soc. 58 (1936) 516–522. doi:10.1021/ja01294a036.

[38] A. Ambrus, D. Chen, J. Dai, T. Bialis, R.A. Jones, D. Yang, Human telomeric sequence forms a hybrid-type intramolecular G-quadruplex structure with mixed parallel/antiparallel strands in potassium solution, Nucleic Acids Res. 34 (2006) 2723–2735. doi:10.1093/nar/gkl348.

[39] L. Petraccone, C. Spink, J.O. Trent, N.C. Garbett, C.S. Mekmaysy, C. Giancola, J.B. Chaires, Structure and stability of higher-order human telomeric quadruplexes, J. Am. Chem. Soc. 133 (2011) 20951–20961. doi:10.1021/ja209192a.

[40] E. Michelucci, G. Pieraccini, G. Moneti, C. Gabbiani, A. Pratesi, L. Messori, Mass spectrometry and metallomics: a general protocol to assess stability of metallodrug-protein adducts in bottom-up MS experiments, Talanta. 167 (2017) 30–38. doi:10.1016/j.talanta.2017.01.074.

[41] T. Marzo, D. Cirri, C. Gabbiani, T. Gamberi, F. Magherini, A. Pratesi, A. Guerri, T. Biver, F. Binacchi, M. Stefanini, A. Arcangeli, L. Messori, Auranofin, Et$_3$PAuCl, and Et$_3$PAuI are highly cytotoxic on colorectal cancer cells: a chemical and biological study, ACS Med. Chem. Lett. 8 (2017) 997–1001. doi:10.1021/acsmedchemlett.7b00162.

[42] J.N. Burstyn, W.J. Heiger-Bernays, S.M. Cohen, S.J. Lippard, Formation of cis-diamminedichloroplatinum(II) 1,2-intrastrand cross-links on DNA is flanking-sequence independent, Nucleic Acids Res. 28 (2002) 4237–4243. doi:10.1093/nar/28.21.4237.

[43] K.M. Comess, C.E. Costello, S.J. Lippard, Identification and characterization of a novel linkage isomerization in the reaction of trans-diamminedichloroplatinum(II) with 5′-d(TCTACGCGTTCT), Biochemistry. 28 (1990) 2102–2110. doi:10.1021/bi00460a020.

[44] S.J. Lippard, Platinum DNA Chemistry, in: Platin. Other Met. Coord. Compd. Cancer

Chemother., Howell S.B, Springer, Boston, MA, 1991: pp. 1–12. doi:https://doi.org/10.1007/978-1-4899-0738-7_1.

[45] W. Zeng, Y. Zhang, W. Zheng, Q. Luo, J. Han, J. Liu, Y. Zhao, F. Jia, K. Wu, F. Wang, Discovery of cisplatin binding to thymine and cytosine on a single-stranded oligodeoxynucleotide by high resolution FT-ICR mass spectrometry, Molecules. 24 (2019) 1852. doi:10.3390/molecules24101852.

[46] K. Suntharalingam, O. Mendoza, A.A. Duarte, D.J. Mann, R. Vilar, A platinum complex that binds non-covalently to DNA and induces cell death via a different mechanism than cisplatin, Metallomics. 5 (2013) 514–523. doi:10.1039/c3mt20252f.

[47] C. Riccardi, D. Musumeci, C. Irace, L. Paduano, D. Montesarchio, Ru(III) complexes for anticancer therapy: the importance of being nucleolipidic, Eur. J. Org. Chem. 2017 (2017) 1100–1119. doi:10.1002/ejoc.201600943.

[48] M. Poursharifi, M.T. Wlodarczyk, A.J. Mieszawska, Nano-based systems and biomacromolecules as carriers for metallodrugs in anticancer therapy, Inorganics. 7 (2019) 2. doi:10.3390/inorganics7010002.
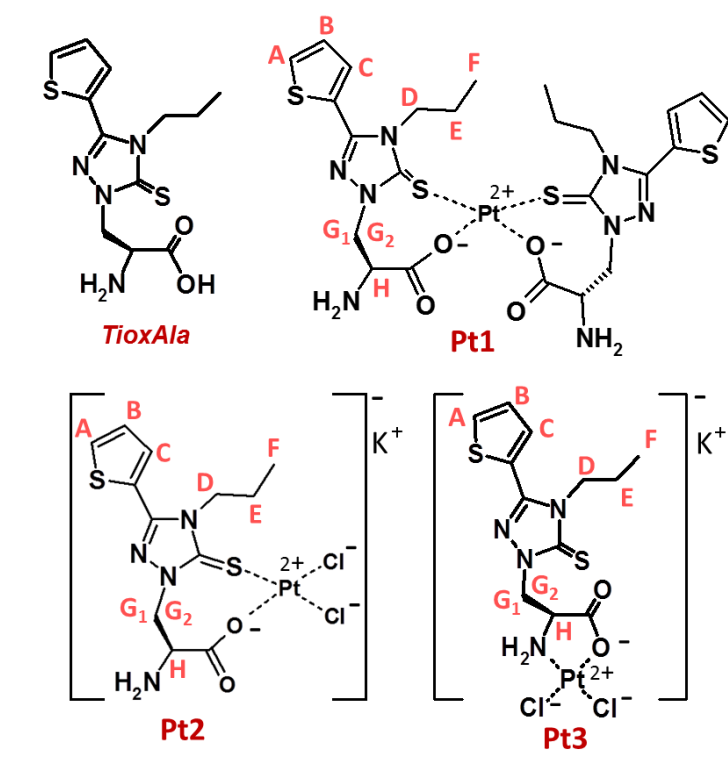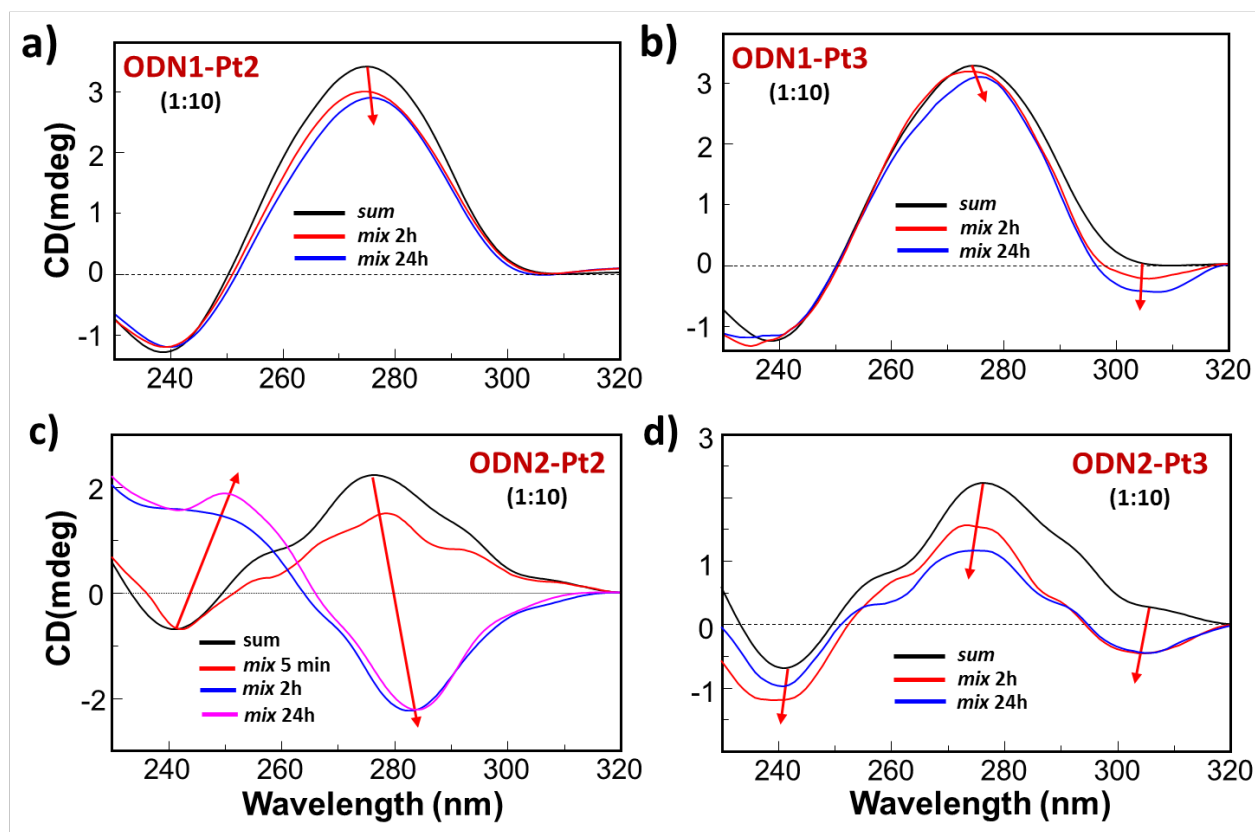
Figure 1: Molecular structure of the artificial amino acid, here named *TioxAla*, based on L-alanine derivatized with a triazolyl-thione group and a thiophenyl moiety. Structures assigned to the three novel complexes **Pt1**, **Pt2** and **Pt3** with the symbolism used for the NMR assignments.

Figure 2: MALDI-TOF mass spectra (positive ion-mode) of **Pt1** (**a**), **Pt2** (**b**) and **Pt3** (**c**), obtained using α-cyano-hydroxycinnamic acid (CHCA) as matrix.

| | a) | | b) |
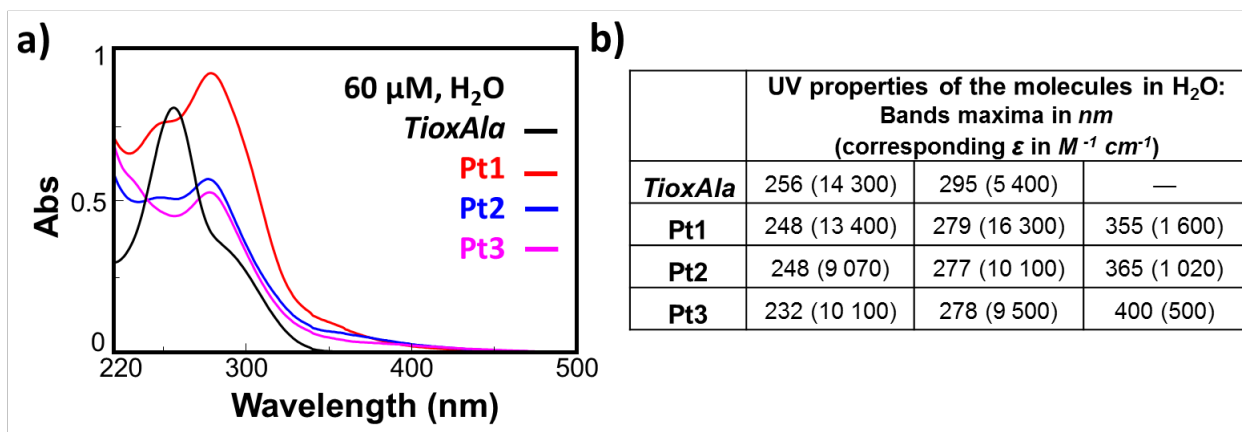
Figure 3: **a**) Overlapped UV-vis spectra of *TioxAla*, **Pt1**, **Pt2** and **Pt3** dissolved in H_2O at 60 μM concentration; **b**) Absorption features of the three platinum complexes and the starting amino acid dissolved in H_2O. Molar extinction coefficients (ε) were calculated from the slopes of standard calibration curves, constructed using Beer's law.
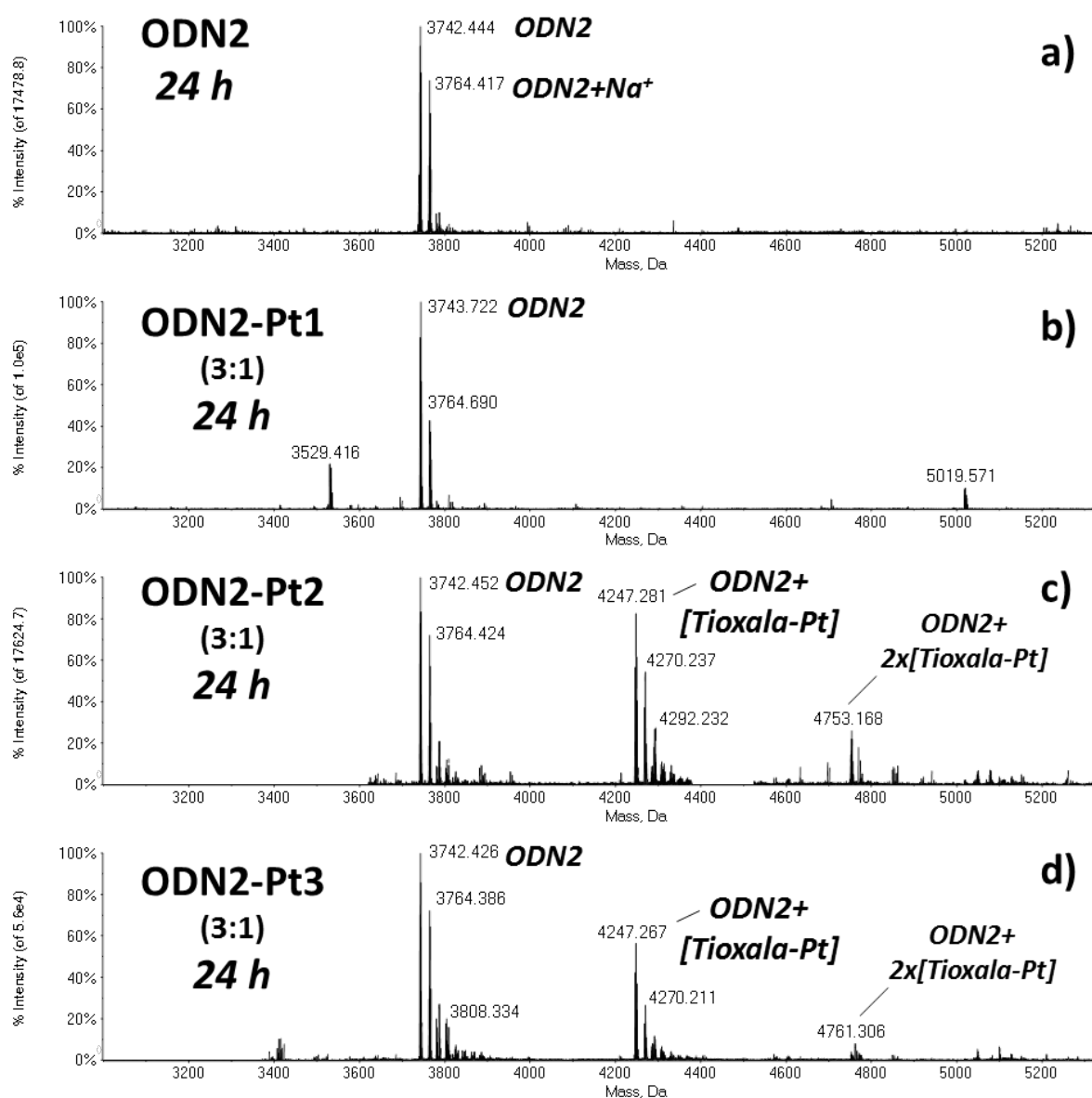
Figure 4: CD-monitored binding experiments with the single stranded random coil ODNs. CD spectra of 4 μM solutions of **ODN1** (**a**,**b**) or **ODN2** (**c**,**d**) with 10 equiv. **Pt2** (**a**,**c**) and **Pt3** (**b**,**d**), recorded in a two-chambers cell before (*sum*) and after mixing (*mix*) the solutions of the two systems at different times, in 50 mM KCl, 10 mM Na_2HPO_4/NaH_2PO_4, pH = 7.2.
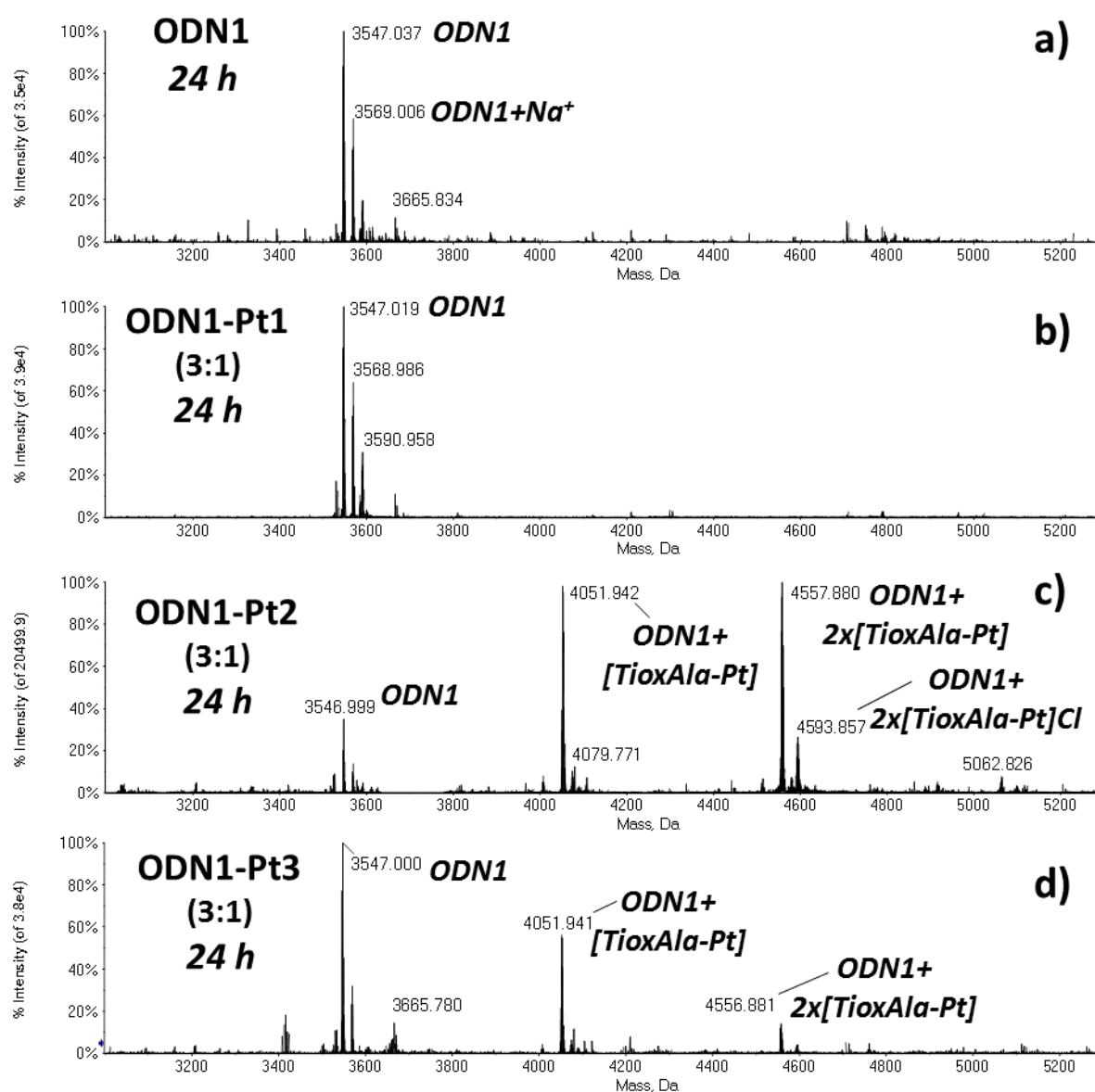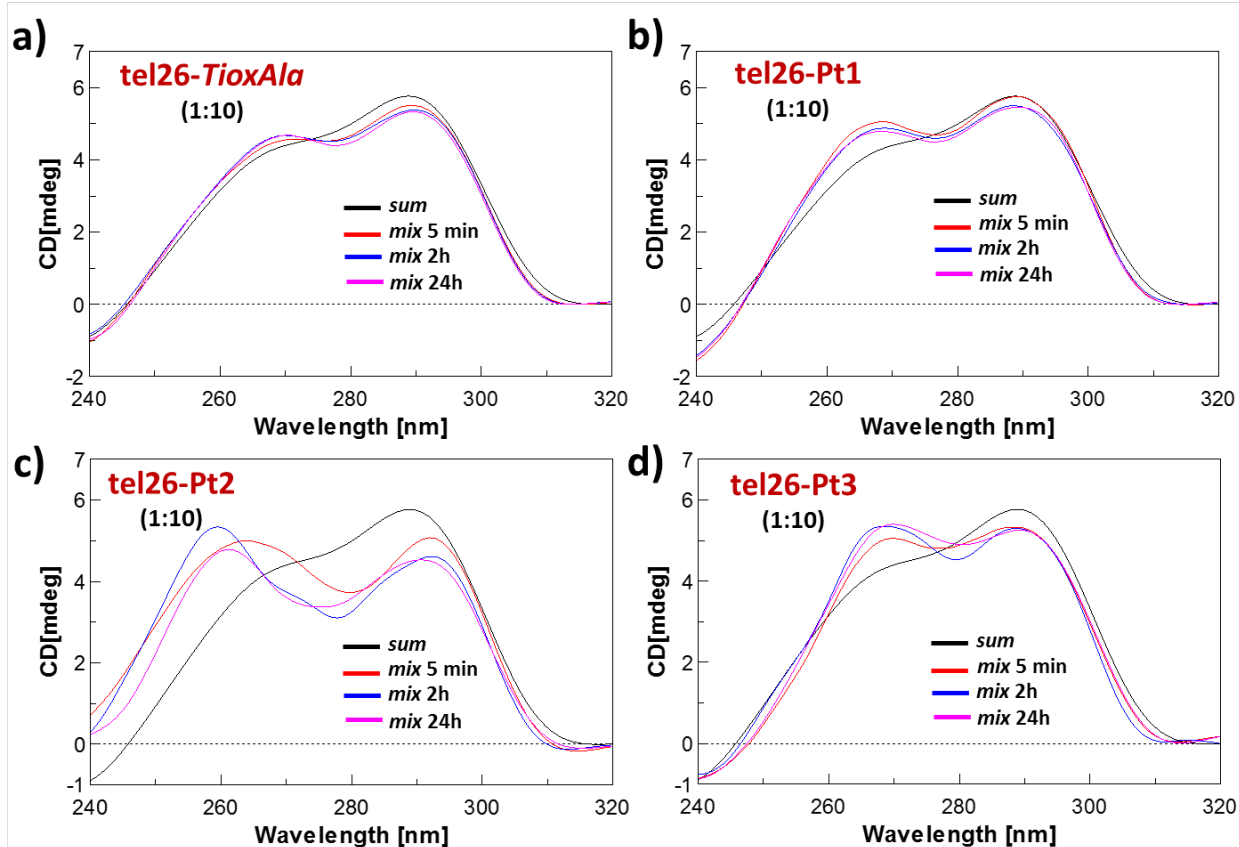
Figure 5: Deconvoluted ESI mass spectra of **ODN1** (6 μM solution) in water (**a**) and incubated at 37 °C for 24 h with **Pt1** (**b**), **Pt2** (**c**), and **Pt3** (**d**) at 3:1 metal to ODN molar ratio.
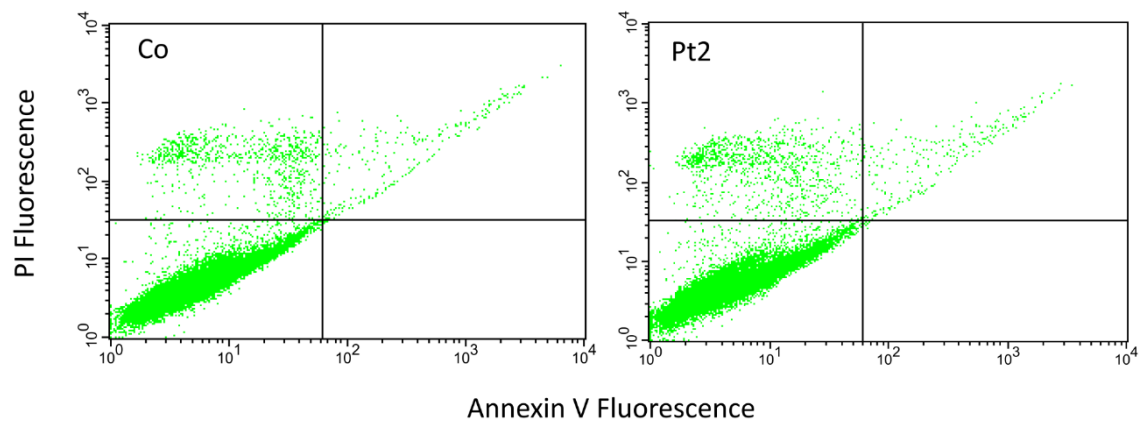
Figure 6: Deconvoluted ESI mass spectra of **ODN2** (6 µM solution) in water (**a**) and incubated at 37 °C for 24 h with **Pt1** (**b**), **Pt2** (**c**), and **Pt3** (**d**) at 3:1 metal to ODN molar ratio.

Figure 7: CD-monitored binding experiments with the G-quadruplex DNA. CD spectra of tel$_{26}$ G4 (4 μM) and the various compounds (10 equiv. each), *TioxAla* (**a**), **Pt1** (**b**), **Pt2** (c) and **Pt3** (**d**), recorded in a two-chambers cell before (*sum*) and after mixing (*mix*) the solutions of the two systems at different times, in 50 mM KCl, 10 mM Na$_2$HPO$_4$/NaH$_2$PO$_4$, pH = 7.2.
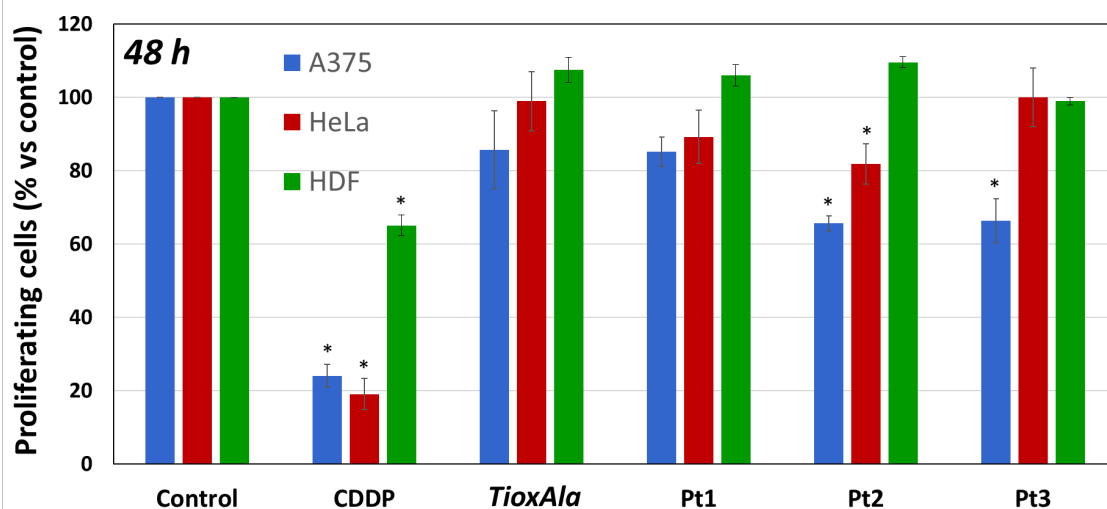
Figure 8: Cells were incubated with 50 μM Pt(II) complexes, *TioxAla* or 10 μM CDDP for 48 h. The results are presented as percentage of proliferating cells with respect to the control (vehicle treated cells) and are expressed as means ± SE of three independent experiments (* $p < 0.05$).

Figure 9: Apoptosis analyses with annexin V-FITC/PI double staining on A375 cells. Untreated cells (Co); **Pt2** treated cells (Pt2); Upper left quadrant: necrotic cells; upper right: advanced apoptotic cells; lower left: viable cells; lower right: early apoptotic cells. These pictures are representative of three independent experiments.